Aus dem Experimental and Clinical Research Center
der Medizinischen Fakultät Charité – Universitätsmedizin Berlin

DISSERTATION

Kardiovaskuläre Magnetresonanztomographie in der klinischen Routine
-
Etablierung zeiteffizienter Ansätze

zur Erlangung des akademischen Grades
Doctor medicinae (Dr. med.)

vorgelegt der Medizinischen Fakultät
Charité – Universitätsmedizin Berlin

von

Stephanie Wiesemann (geb. Funk)

aus Freiburg i. Br.

Datum der Promotion: 23.06.2019

Abstrakt

Die zunehmende Bedeutung der kardiovaskulären Magnetresonanztomographie zur Diagnostik und Therapiesteuerung findet sich auch in den aktuellen Leitlinien der Kardiologie wieder. Dennoch ist ihre Anwendung noch nicht so routinemäßig verfügbar, wie es sich anbieten würde. Als ein limitierender Faktor gilt hierbei die Untersuchungsdauer.
Für eine zeiteffizientere Untersuchung ist eine Nutzung bereits vorhandener Routineaufnahmen für weitere Fragestellungen sinnvoll. Gleichzeitig müssen neu entwickelte, schnellere Techniken validiert werden. Nur so können die Möglichkeiten der kardialen Magnetresonanztomographie, insbesondere die einzigartige Möglichkeit zur nicht-invasiven Gewebedifferenzierung, künftig eine breitere Anwendung finden.
Ziel dieser Arbeit ist es, Möglichkeiten zur effizienteren und schnelleren Untersuchung aufzuzeigen, um die Möglichkeiten der kardialen Magnetresonanztomographie innovativ und in breiterer Anwendung nutzbar zu machen.

Bei 203 gesunden Probanden wurde der linke Vorhof analysiert, um Normwerte basierend auf einem zeitsparenden klinischen Routineprotokoll zu erstellen. Abhängigkeiten von Alter, Geschlecht und Feldstärke wurden aufgezeigt.[1]
Des weiteren wurden zwei neue, schnellere Aufnahmetechniken zur Narbendarstellung bei 312 Patienten mit verschiedenen Pathologien anhand des Vergleichs zur Referenzstandardsequenz evaluiert.[2] Außerdem wurden 23 Sarkompatienten vor und im Laufe ihrer Anthrazyklin-Therapie wiederholt untersucht, um einen potentiellen Markers einer anthrazyklin-induzierten Kardiomyopathie zu ermitteln.[3]

Die Evaluierung der Normwerte des linken Vorhofs ergab einen Unterschied zwischen den Geschlechtern bezüglich der absoluten Volumina des linken Vorhofs. Dieser Unterschied war nicht mehr erkennbar nach Normierung der Werte auf Body-Surface-Area oder Körpergröße. Die Feldstärke hatte keinen Einfluss. Das enddiastolische Volumen des linken Vorhofs nahm mit zunehmendem Alter ab.[1]
Die neuen Aufnahmetechniken hatten eine signifikant kürzere Aufnahmezeit und erlaubten darüber hinaus auch eine Auswertung bei Patienten mit arrhythmischem

Herzschlag. Alle 201 in der Referenzstandardsequenz positiven Befunde wurden ebenfalls mit einer der neuen Aufnahmetechniken erkannt. In der anderen neuen Aufnahmetechnik wurden zwei kleine Narben (<1g) übersehen.[2]
Sarkompatienten, die nach Beendigung der Anthrazyklintherapie eine anthrazyklin-induzierte Kardiomyopathie entwickelten, zeigten bereits 48h nach Therapiebeginn myokardiale Gewebeveränderungen, welche sich bis zum Ende der Therapie wieder erholten.[3]

Zusammenfassend konnten durch die Etablierung von Normwerten des linken Vorhofs anhand eines zeitsparenden Routineprotokolls sowie der Validierung zeitsparender Aufnahmen zur Narbendarstellung Ansätze zur zeiteffizienteren und schnelleren Durchführung einer kardialen Magnetresonanztomographieuntersuchung gezeigt werden, durch die perspektivisch zeiteffizientere Untersuchungen möglich sind und somit eine breitere Anwendung auch innovativ zur Prädiktion von Kardiomyopathien möglich macht.

Abstract

The increasing importance of cardiovascular magnetic resonance for diagnostics and therapy guiding is reflected in current guidelines of cardiology. The clinical application, however, is not as widely spread as could be expected from that. The length of the examination is often seen as one limitation.
For a more time-efficient examination the use of already acquired images for additional information is sensible. Also, newly developed, faster sequences have to be validated for future routine use. Thereby the potential of cardiovascular magnetic resonance, especially the unique possibility of non-invasive myocardial tissue differentiation, can be spread more broadly.
Aim of this work is to show possibilities for a more efficient and faster examination to use the full potential of cardiovascular magnetic resonance also innovatively and for a broader spectrum.

Left atria of 203 healthy volunteers were analyzed to establish normal values based on a time-efficient clinical routine protocol. Influence of age, sex and field strengths was evaluated.[1]
Additionally, two new, faster acquisition techniques for scar imaging were compared to a reference standard sequence in 312 patients with different pathologies.[2]
Furthermore 23 patients with sarcoma were examined before, during and after their anthracyclin-therapy to find a potential marker of anthracyclin-induced cardiomyopathy.[3]

Evaluation the newly established normal values of the left atria showed a significant difference of the absolute volumes between both sexes, which could not be observed anymore after adjusting to body-surface-area or height. Field strength did not influence the results. The enddiastolic volume of the left atria decreased with age.[1]
The new acquisition techniques had a significantly shorter acquisition time and additionally allowed for evaluation in patients with arrhythmia. All 201 positive results as depicted by the standard reference sequence were also detectable by one technique. With the other technique two small scars (<1g) were missed.[2]
Patients with sarcoma, who developed an anthracyclin-induced cardiomyopathy after the anthracyclin-therapy, already showed 48 hours after beginning of treatment

changes in myocardial tissue differentiation, which recovered until the end of the therapy.[3]

In summary by establishing normal values for the left atria in a fast routine protocol and by validating newer, faster techniques for scar detection approaches for a more time-efficient and faster application of cardiovascular magnetic resonance could be shown, which will help expanding the application also to innovatively predict cardiomyopathies.

1. Einleitung

1.1 Die Magnetresonanztomographie allgemein und Besonderheiten der kardiovaskulären Magnetresonanztomographie

Die Magnetresonanztomographie (MRT) nimmt eine zentrale Rolle in der medizinischen Bildgebung ein. Ein Alleinstellungsmerkmal der Methode ist, dass sie keine ionisierende Strahlung verwendet und eine freie Wahl der Schnitte durch den menschlichen Körper ermöglicht.

Die Bedeutung der kardiovaskulären MRT in der Diagnostik und Therapiesteuerung kardiovaskulärer und systemischer Erkrankungen hat in den letzten Jahren deutlich zugenommen [4, 5]. Mit verbesserter Auflösung und schnelleren Untersuchungstechniken ist sie, insbesondere auf Grund ihrer Anwendung ohne ionisierende Strahlung, zu einem wichtigen Werkzeug in der klinischen Routine geworden.

So gilt sie mittlerweile als Goldstandard für die Evaluierung der kardialen Funktion [6-8]. Auch bei der Detektion ischämischer und nicht-ischämischer kardialer Erkrankungen spielt sie eine wichtige Rolle. Es konnte gezeigt werden, dass die kardiovaskuläre MRT im Vergleich zur Einzelphotonen-Emissionscomputertomographie (single photon emission computed tomography = SPECT) zum nicht-invasiven Nachweis von Perfusionsminderungen des Herzmuskels überlegen ist [9].

Ebenso wird sie bereits erfolgreich bei der Detektion inflammatorischer Prozesse eingesetzt [10]. Hier spielt die Möglichkeit zur nicht-invasiven Gewebedifferenzierung eine große Rolle; so kann zum Beispiel bei der Myokarditis oder im Rahmen von Systemerkrankungen zur Diagnosestellung auf invasive Methoden verzichtet werden.

Allerdings wird sie bisher in der klinischen Routine noch weniger eingesetzt, als es ihre diagnostischen Möglichkeiten anbieten würden. Ein limitierender Faktor ist hierbei die Untersuchungsdauer. Abhängig von der Indikation und der Erfahrung des Untersuchers dauert eine kardiovaskuläre MRT-Untersuchung durchschnittlich ca. 1 Stunde.

1.2 Normwertetablierung in der kardiovaskulären Magnetresonanztomographie

Ein weiteres Hindernis der flächendeckenden kardiovaskulären MRT-Anwendung ist das Fehlen von Erfahrungs- und Normwerten in einigen Bereichen. Als Goldstandard

gilt sie bereits für die Quantifizierung der linksventrikulären (LV) Volumina und Funktion [6-8]. Auch für die Quantifizierung der Vorhöfe gibt es bereits Erfahrungswerte [11-15]. Diese basieren jedoch auf eigens angepassten Vorhofaufnahmen und werden somit oft in der klinischen Routine aus Zeitersparnisgründen ausgelassen.

Ein Teil dieser kumulativen Dissertationsarbeit ist die Etablierung von Normwerten für die Volumina und Funktion des linken Vorhofs (LA) basierend auf einem zeitsparenden Routineprotokoll.

Auch sind mittlerweile einige Sequenzen technisch so weiterentwickelt worden, dass sie in kürzerer Zeit mehr Informationen liefern können. Zur Darstellung kardialer Narben werden bisher üblicherweise 10-12 einzelne Schichten aufgenommen. Die Aufnahme erfolgt nach Kontrastmittelgabe (Late-Gadolinium-Enhancement = LGE). Hier können Narben nach abgelaufenem Myokardinfarkt, Myokarditisnarben und Fibrosen (zum Beispiel bei Kardiomyopathien oder Systemerkrankungen) dargestellt werden und somit das kardiale Gewebe differenziert werden. Die Gesamtabdeckung des linken Ventrikels dauert mit dieser Standardsequenz durchschnittlich ca. 10 Minuten.

Neue technische Ansätze ermöglichen nun eine wesentlich schnellere Aufnahmezeit. Einer davon umfasst sogenannte „Multislice“-Aufnahmen. Mittels Multislice-LGE-Aufnahmen kann das ganze Herz in einer Aufnahme akquiriert werden [16, 17].

Ein zusätzlicher Vorteil ist, dass die Probanden hierbei frei atmen können, da die Atmung separat registriert wird [17]. Sie müssen nicht, wie in der Standardsequenz, für jede der 10-12 Schichten ca. 15 Sekunden die Luft anhalten. Entsprechend kann die Bildakquise mit der Multislice-Technik vor allem bei Patienten mit Problemen beim Atemanhalten, also insbesondere schwer kranke Patienten, deutlich vereinfacht werden.

Diese Sequenzen waren bisher nicht klinisch validiert, entsprechend besteht die Befürchtung, insbesondere kleinere Narben/Fibrosen zu übersehen.

Ein Teil dieser kumulativen Dissertationsarbeit ist die klinische Validierung neuer Multislice-LGE-Aufnahmen.

1.3 Klinische Anwendbarkeit der kardiovaskulären Magnetresonanztomographie

Nicht nur durch diese kontrastmittelverstärkten LGE-Bilder können Narben und Fibrosen nachgewiesen werden, sondern neuerdings auch durch andere Techniken.

Insbesondere durch das parametrische Mapping kann das Gewebe weiter differenziert werden. Während LGE-Aufnahmen erst die Spätschäden im Gewebe darstellen, kann mittels parametrischem Mapping bereits eine frühe Detektion von anderweitig noch nicht erkennbaren Myokardschäden erfolgen. Zusätzlich kann hier eine genaue Quantifizierung erfolgen.

Es konnte bereits gezeigt werden, dass die Anthrazyklin-Therapie bei Patienten mit unterschiedlichen Krebserkrankungen die Entwicklung von Spätschäden des kardialen Gewebes im Sinne von diffuser myokardialer Fibrose Jahre nach der Therapie begünstigt. Da die Überlebenswahrscheinlichkeit der meisten Krebserkrankten im Laufe der letzten Jahrzehnte deutlich gestiegen ist [18], werden diese Nebeneffekte der Chemotherapie immer wichtiger. Anthrazykline haben häufig kardiale Nebenwirkungen, welche letztendlich zur Herzinsuffizienz, der anthrazyklininduzierten Kardiomyopathie (aKMP), führen können [19].

Durch die kardiovaskuläre MRT besteht nun die Möglichkeit zur weiteren Gewebedifferenzierung und zur Früherkennung kardialer Gewebeschäden.

Bisher wurden zwar die Spätschäden im Sinne von myokardialen Narben und Fibrosen und ihr Einfluss auf die Entwicklung einer Herzinsuffizienz beschrieben, dies kann jedoch erst nach Beendigung der Chemotherapie erfolgen und hat damit bisher keinen direkten, prädiktiven Vorteil für die Patienten unter Chemotherapie [20, 21].

Die Möglichkeit der frühzeitigen Erkennung von Gewebeveränderungen zur Prädiktion späterer kardiotoxischer Effekte mittels kardiovaskulärer MRT bei Patienten unter Anthrazyklin-Therapie ist ebenfalls Teil der kumulativen Dissertationsarbeit.

1.4 Zielstellung der Arbeit

Ziel der dissertationsrelevanten Studien ist es, eine Möglichkeit zeiteffizienter Darstellung von kardialer Morphologie und Gewebeschäden zu zeigen, um dadurch die neuen Möglichkeiten zur kardialen Gewebedifferenzierung innovativ zur Prädiktion nutzbar zu machen.

2. Methodik

2.1 Normwertetablierung der Volumina und Funktion des linken Vorhofs

2.1.1 Studienaufbau und MRT-Scan-Protokoll

Es wurden 203 gesunde Probanden analysiert. 111 Untersuchungen wurden bei 1,5 Tesla (T) (Magnetom Avanto, Siemens Healthcare, Erlangen) durchgeführt, 92 Untersuchungen bei 3,0 T (Magnetom Verio, Siemens Healthcare, Erlangen). In zwei langen Achsen (2-Kammerblick und 4-Kammerblick) wurden routinemäßige steady-state free precession (SSFP) cine Aufnahmen durchgeführt.[1]

Bei 1,5 T waren die Sequenzparameter: Repetitionszeit (repetition time =TR) 2,8 ms, Schichtdicke 6 mm, Flipwinkel 80 Grad, Echozeit (echo time = TE) 1,2 ms, Sichtfeld (field of view = FOV) 276 x 340 mm^2, Matrix 156 x 192, rekonstruiert zu 1,77 mm x 1,77 mm, 30 Herzphasen.[1]

Bei 3,0 T waren die Sequenzparameter: TR 3,1 ms, Schichtdicke 6 mm, Flipwinkel 45 Grad, TE 1,3 ms, FOV 276 x 340 mm^2, Matrix 156 x 192, rekonstruiert zu 1,77 mm x 1,77 mm, 30 Herzphasen. [1]

2.1.2 Bildanalyse

In die weitere Analyse wurden nur Aufnahmen eingeschlossen, bei denen der linke Vorhof ausreichend dargestellt war. [1]

Die Bildanalyse erfolgte mit der kommerziell erwerblichen Software cvi42® version 5.1 (Circle Cardiovascular Imaging Inc., Calgary, Canada). Die Quantifizierung der LA-Volumina und -Funktion erfolgte in der Systole und Diastole, je im 2- und im 4-Kammerblick. Dabei wurden das Vorhofsohr und die Pulmonalvenen ausgespart. Es wurden das enddiastolische und endsystolische Volumen des linken Vorhofs (LA-EDV bzw. LA-ESV), das Schlagvolumen des linken Vorhofs (LA-SV) und die linksatriale Pumpfunktion (LA-EF) quantifiziert.[1]

In der klinischen Routine werden die LA Endsystole und Enddiastole oft zum selben Zeitpunkt im Herzzyklus und damit im selben Bild wie die LV Enddiastole und Endsystole quantifiziert. Allerdings ist die LA Endsystole oft nicht genau zum identischen Zeitpunkt wie die LV Enddiastole, sondern bereits Millisekunden vorher. In 20 Aufnahmen wurden die Volumina und Funktionsberechnungen aus beiden unterschiedlichen Auswertezeitpunkten miteinander verglichen. Dabei wurde der linksatriale Auswertezeitpunkt zum Zeitpunkt der LV-Diastole „LA Systole 1“ und der

Zeitpunkt der wahren LA Endsystole „LA Systole 2“ genannt. Entsprechend verglichen wir auch die Zeitpunkte der Auswertung der LA-Diastole, „LA Diastole 1“ entspricht dem Zeitpunkt der LV-Systole und „LA Diastole 2“ dem Zeitpunkt der wahren LA Enddiastole.[1]

2.1.3 Statistische Analyse

Es wurden die Mittelwerte und Standardabweichung für LA-EDV, LA-ESV, LA-SV und LA-EF berechnet. Alle Werte wurden zusätzlich auf die Körperoberfläche (Body-surface-area = BSA) und die Körpergröße (height = H) bezogen.[1]
Wir analysierten die Unterschiede zwischen den Feldstärken sowie den Altersverlauf der Volumina und Funktion. [1]

2.2 Darstellung myokardialer Narben mittels Late-Gadolinium-Enhancement durch unterschiedliche Sequenzen

Nach Kontrastmittelgabe können mittels kardiovaskulärer MRT Narben und Fibrosen im LGE nachgewiesen werden. Dafür gibt es standardmäßig bisher eine segmentierte Phasen-sensitive Inversionswiederherstellung (phase sensitive inversion recovery = PSIR) Sequenz mit der der linke Ventrikel in mehreren (üblicherweise 10-12) kurzen Achsen dargestellt wird. Für jede Kurzachsenschicht wird eine ca. 10-15 Sekunden andauernde Aufnahme mit Atemanhalte durchgeführt. Neue Multislice-Sequenzen ermöglichen eine schnellere Aufnahme und/oder eine Aufnahme ohne Atemanhalte.[2]

2.2.1 Vergleich der Sequenzen bei Patienten mit ischämischen und nicht-ischämischen Kardiomyopathien

In dieser prospektiven Studie verglichen wir die standardmäßig akquirierten PSIR LGE Aufnahmen mit zwei verschiedenen Multislice-LGE-Aufnahmen mit und ohne Atemanhalte bei Patienten mit ischämischen und nicht-ischämischen Kardiomyopathien.[2]

2.2.2 Studienaufbau und MRT-Scan-Protokoll

Es wurden 312 Patienten prospektiv eingeschlossen. Bei allen Patienten bestand eine klinische Indikation zur kardiovaskulären MRT-Untersuchung.[2]
Von diesen hatten 212 Patienten eine koronare Herzerkrankung (KHK), 53 eine hypertrophe Kardiomyopathie (HCM) und 47 eine inflammatorische Herzerkrankung.
Bei allen Patienten wurde eine kardiovaskuläre MRT-Untersuchung bei 1,5 T (Magnetom Avanto Fit, Siemens Healthcare, Erlangen) mit drei verschiedenen LGE Sequenzen durchgeführt:

- eine segmentierte, single-slice, single-breathhold zweidimensionale (2D) fast low angle shot (FLASH) basierte PSIR (FLASH-PSIR) (Referenzstandard)
- eine multislice 2D bSSFP basierte inversion recovery Sequenz (bSSFP-IR)
- eine multislice 2D bSSFP basierte PSIR Sequenz (bSSFP-PSIR)

Die bSSFP-PSIR Sequenz wurde einmal in Atemanhalte und einmal in freier Atmung aufgenommen, alle übrigen Sequenzen wurden in Atemanhalte aufgenommen.
Die Sequenzen wurden in zufälliger Reihenfolge aufgenommen.[2]

2.2.3 Bildanalyse

Zunächst wurde die Bildqualität aller Aufnahmen beurteilt. Dies erfolgte einerseits nach visueller Einschätzung und andererseits mittels Contrast-to-Noise Ratio (CNR). Anschließend wurde das Vorhandensein von LGE sowohl visuell als auch quantitativ beurteilt.[2]

Die quantitative Auswertung der Narbengröße erfolgte schwellenwert-basiert. Hierbei wurden in alle Aufnahmen der Narbendarstellung die endo- und epikardialen Konturen des Myokards umfahren und Regions Of Interest (ROIs) im gesunden Myokard und im Myokard mit LGE eingezeichnet. Eine wahre Narbe, also positives LGE, wurde bei Patienten mit KHK als eine Signalintensität, die 6 Standardabweichungen über dem gesunden Myokard lag, definiert und bei Patienten mit HCM oder inflammatorischer Herzerkrankung als 3 Standardabweichungen über dem gesunden Myokard. Anschließend wurde die Narbenmasse errechnet und die errechneten Massen zwischen den Sequenzen verglichen.[2]
Die Bildanalyse wurde mit cvi42® version 4.2 (Circle Cardiovascular Imaging Inc., Calgary, Canada) durchgeführt.[2]

2.3 Gewebedifferenzierung zur Vorhersage der Entwicklung einer anthrazyklin-induzierten Kardiomyopathie

2.3.1 Studienaufbau und MRT-Scan-Protokoll

Es wurden 30 Patienten prospektiv eingeschlossen. Alle Patienten hatten ein histologisch bestätigtes Weichteilsarkom und bei allen Patienten war eine Anthrazyklin-Therapie mit einer kumulativen Dosis von 360-400mg/m^2 geplant. [3]

Bei allen Patienten wurden drei kardiovaskuläre MRT- Untersuchungen bei 1,5 T (Magnetom Avanto Fit, Siemens Healthcare, Erlangen) durchgeführt. Die erste Untersuchung wurde innerhalb von 48 Stunden vor Beginn der Anthrazyklin-Therapie durchgeführt, die zweite 48 Stunden nach der Erstgabe des Medikaments und die dritte vier Wochen nach der letzten Gabe.[3]

Zur Bestimmung der kardialen Funktion wurden SSFP-cine Aufnahmen durchgeführt. Zur Gewebedifferenzierung erfolgten T1 und T2 Mapping Aufnahmen. Hierfür wurde für die T1 Mapping Aufnahme eine modified Look-Locker inversion recovery (MOLLI) Sequenz in einer mittventrikulären Schicht vor und 15 Minuten nach Gabe von 0,2mmol/kg Körpergewicht Gadoteridol Kontrastmittel (ProHance®, Bracco Diagnostics, Princeton, New Jersey, USA) durchgeführt. [3]

Für das T2 Mapping wurde eine etablierte T2 gewichtete SSFP Technik in 3 Schichten angewendet. Abschließend erfolgte die Narbendarstellung in Standard-LGE-Aufnahmen.[3]

2.3.2 Bildanalyse

Die Bildanalyse wurde mit cvi42® version 4.2 (Circle Cardiovascular Imaging Inc., Calgary, Canada) durchgeführt. Die links- und rechtsventrikuläre Funktion und -Masse wurden in kurzen Achsen ausgewertet, atriale Volumina in 4- und 2-Kammerblick. T1 und T2 Mapping wurden in einer mittventrikulären kurzen Achse ausgewertet. Relatives und absolutes Extrazelullärvolumen (ECV) wurde mittels kontrastmittelfreier und kontrastmittelverstärkter T1-Werte und dem Hämatokrit berechnet. LGE wurde von zwei unabhängigen Auswertern visuell hinsichtlich Ort und Transmuralität bewertet.[3]

Inter- und Intraobservervariabilität wurden in einer Subgruppe von 10 Patienten analysiert.[3]

Ein Abfall der LV-EF um mehr als 10% wurde nach aktuellen Guidelines als die Entwicklung einer aKMP definiert. [3]

3. Ergebnisse

3.1 Normwertetablierung der Volumina und Funktion des linken Vorhofs

Bei 21 Probanden war die Darstellung des LA unzureichend, so dass sie von der weiteren Analyse ausgeschlossen werden mussten. 182 Probanden wurden analysiert. Davon wurden 89 bei 3,0 T und 93 bei 1,5 T untersucht (s. Tabelle 1).[1]

	1.5 Tesla (Mittelwert ± Standardabweichung (Minimum / Maximum))	3.0 Tesla (Mittelwert ± Standardabweichung (Minimum / Maximum))
N (gesamt)	93	87
Alter (Jahre)	38 ± 14 (19 / 70)	52 ± 15 (21 / 76)
Körpergröße (cm)	175 ± 9 (153 / 197)	171 ± 11 (118 / 193)
Körpergewicht (kg)	72 ± 12 (48 / 105)	77 ± 15 (53 / 116)
Body-Mass-Index (kg/m^2)	23 ± 3 (18 / 30)	26 ± 7 (17 / 35)
BSA (m^2)	1.9 ± 0.2 (1.5 / 2.4)	1.5 ± 0.6 (0.6 / 2.4)
Pulsfrequenz (Schläge pro Minute)	71 ± 13 (37 / 118)	70 ± 11 (46 / 102)
Systolischer Blutdruck (mmHg)	126 ± 15 (105 / 185)	133 ± 13 (107 / 186)
Diastolischer Blutdruck (mmHg)	75 ± 8 (63 / 94)	76 ± 12 (47 / 109)
LV-EF (%)	63 ± 4 (55 / 75)	63 ± 5 (51 / 77)

Tabelle 1 Charakteristika der gesunden Probanden (übersetzt aus [1])

3.1.1 Unterschiede der Werte in Abhängigkeit von Feldstärke, Alter und Geschlecht

Es gab keinen signifikanten Unterschied der absoluten Volumina zwischen den verschiedenen Feldstärken (LA-EDV: 1,5T 68 ± 19 ml vs. 3,0T 64 ± 18 ml (p=0,19); LA-ESV: 1,5T 23 ± 9 ml vs. 3,0T 23 ± 9 ml (p=0,6); LA-EF: 1,5T 66 ± 7% vs. 3,0T 66 ± 7% (p=0,6)).[1]

Zwischen den absoluten Volumina (LA-EDV und LA-ESV) von Männern und Frauen gab es signifikante Unterschiede. Männer hatten signifikant höhere Werte ($p \leq 0,01$). Wurden diese Werte auf BSA oder Körpergröße normiert, gab es keine signifikanten Unterschiede mehr (s. Abbildung 1 und Tabelle 2). [1]

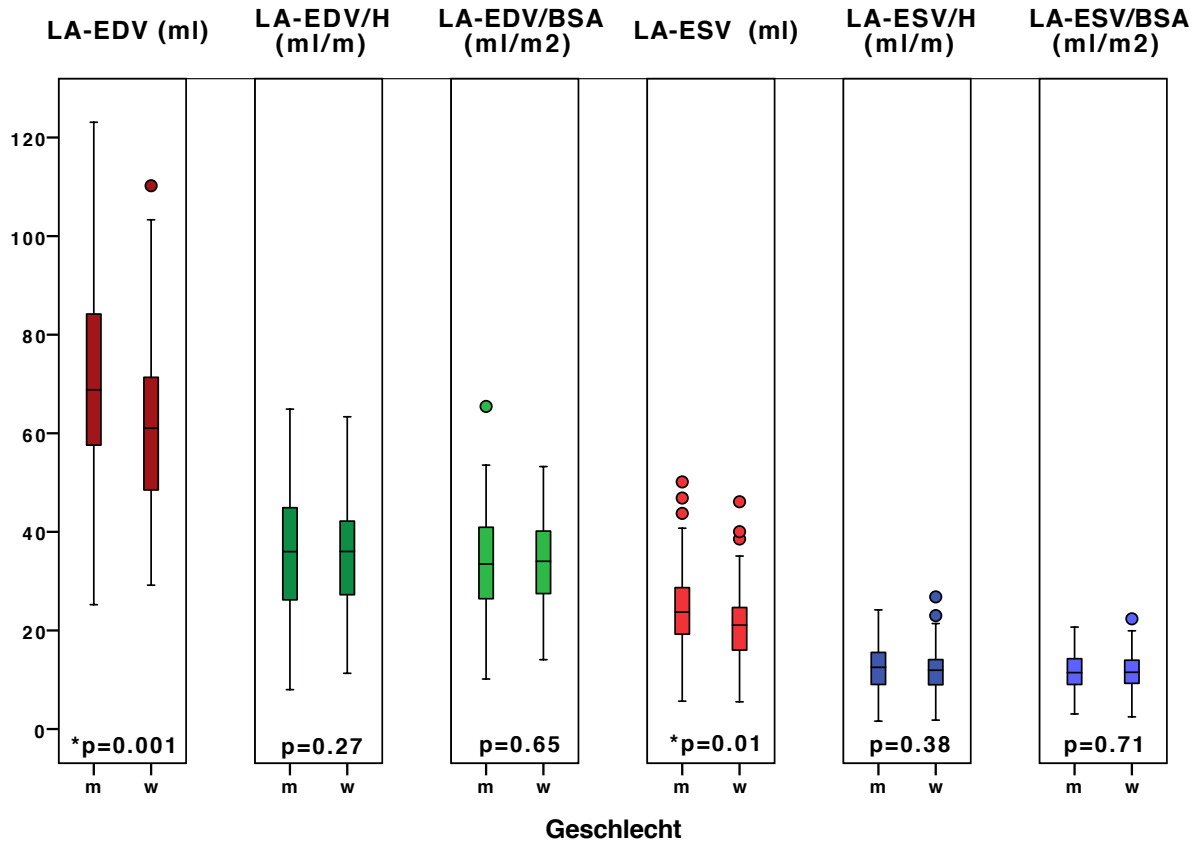

Abbildung 1 Vergleich des LA-EDV und LA-ESV zwischen Männern (m) und Frauen (w). Nach Normierung auf Körperhöhe oder BSA ergibt sich kein signifikanter Volumenunterschied mehr. (übersetzt aus [1])

	Männer (n = 105) (Mittelwert ± Standardabweichung (Minimum / Maximum))	Frauen (n =77) (Mittelwert ± Standardabweichung (Minimum / Maximum))
LA-EDV (ml)	70 ± 19 (25 / 123)	61 ± 16 (29 / 110)
LA-ESV (ml)	24 ± 9 (6 / 50)	21 ± 8 (4 / 46)
LA-SV (ml)	46 ± 13 (17 / 84)	46 ± 9 (24 / 70)
LA-EF (%)	66 ± 7 (50 / 85)	66 ± 8 (48 / 91)
LA-EDV/H (ml/m)	36 ± 12 (8 / 65)	34 ± 12 (11 / 63)
LA-ESV/H (ml/m)	12 ± 5 (2 / 24)	12 ± 5 (2 / 27)
LA-EDV/BSA (ml/m^2)	34 ± 10 (10 / 65)	33 ± 9 (13 / 53)
LA-ESV/BSA (ml/m^2)	12 ± 4 (3 / 21)	11 ± 4 (2 / 22)

Tabelle 2 Referenzwerte des linken Vorhofs für Männer und Frauen (übersetzt aus [1])

Wir fanden einen signifikanten Zusammenhang zwischen Alter und LA-EDV/BSA, wobei LA-EDV/BSA mit zunehmendem Alter abnahm. Der gleiche Zusammenhang bestand zwischen Alter und LA-EDV/H. Diese Abnahme war geschlechtsunabhängig. (s. Abbildung 2).[1]

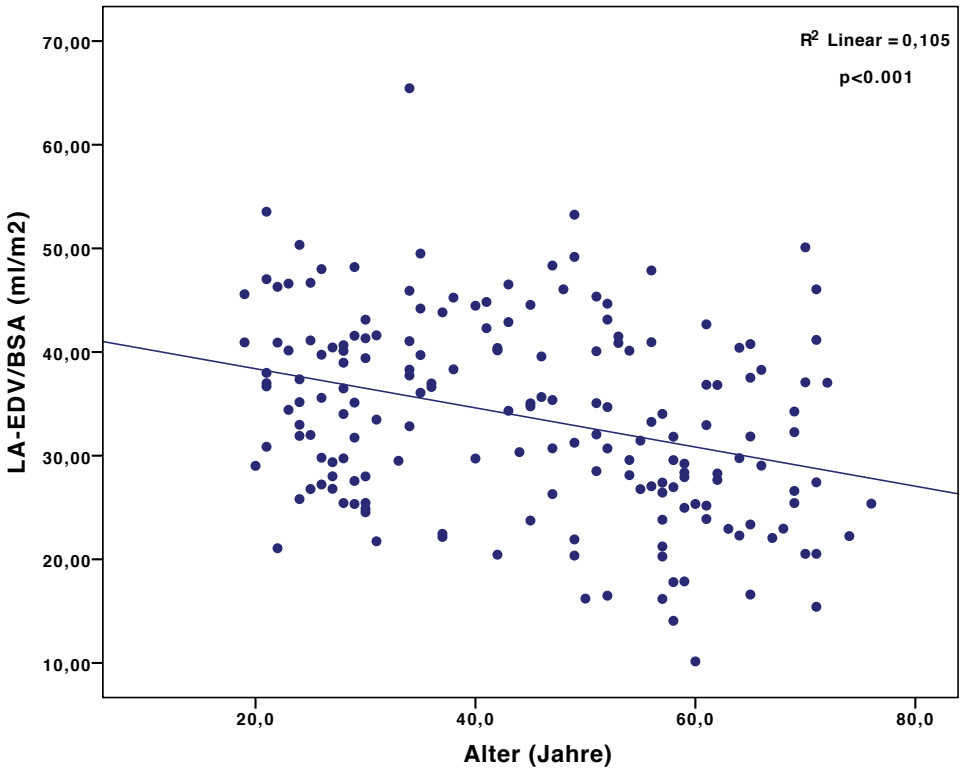

Abbildung 2 Verhältnis von LA-EDV/BSA zu Alter (übersetzt aus [1])

3.1.2 Abhängigkeit der Werte vom Zeitpunkt im Herzzyklus

Die Volumina zum Zeitpunkt von LA-Systole 1 unterschieden sich signifikant von denen zum Zeitpunkt von LA-Systole 2 (LA-ESV: 38 ± 11 ml vs. 28 ± 8 ml, p<0,001), ebenso die Volumina zum Zeitpunkt von LA-Diastole 1 zu Diastole 2 (LA-EDV: 92 ± 21 vs. 74 ± 18 ml, p<0,001). Entsprechend unterschied sich auch LA-EF signifikant (LA-EF: 59 ± 6% vs. 63 ± 7%, p<0,001).[1]

3.2 Vergleich der unterschiedlichen Late-Gadolinium-Enhancement-Sequenzen

Es wurden 312 Patienten eingeschlossen, von denen 14 auf Grund inkompletter MRT-Untersuchungen von der weiteren Analyse ausgeschlossen werden mussten. Von den 298 weiter analysierten Patienten hatten 203 eine KHK, 50 eine HCM und 45 eine inflammatorische Herzerkrankung.[2]

3.2.1 Länge der Aufnahmezeiten

Die Länge der Aufnahmezeit für die Standard-Referenz-Sequenz war signifikant länger als für die Multislice-Aufnahmen (361,5 ± 95,2 s vs. bSSFP-IR 23,4 ± 7,2 s; bSSFP-PSIR 21,9 ± 6,4 s ($p < 0,01$ jeweils)).[2]

3.2.2 Bildqualitätsunterschiede der Sequenzen

Die Bildqualität unterschied sich signifikant zwischen allen Multislice-Sequenzen und der Standard-Referenz-Sequenz. Es gab keinen Einfluss von Erkrankung oder Atemanhalte. Allerdings hatten Arrhythmien einen negativen Einfluss auf die Bildqualität der Standard-Referenz-Sequenz, so dass hier eine nicht-diagnostische Bildqualität bei 48,8% aller Patienten festgestellt wurde. Die Multislice-Sequenzen wurden nicht von Arrhythmien beeinflusst.[2]

Die CNR des Vergleichs von gesundem zu narbigem Myokard war in den bSSFP-PSIR Sequenzen signifikant höher als in der Standard-Referenz-Sequenz ($p < 0,01$) und in der bSSFP-IR Sequenz niedriger ($p < 0,01$).[2]
Die bSSFP-PSIR Sequenz in freier Atmung hatten eine etwas geringere CNR als die Sequenz in Atemanhalte, aber immer noch eine höhere als die Standard-Referenz-Sequenz ($p < 0,01$). [2]
Die Narben eines chronischen Infarktes hatten in allen Sequenzen eine signifikant höhere CNR als bei HCM oder inflammatorischer Herzerkrankung ($p < 0,01$).[2]

3.2.3 Quantitativer und qualitativer Nachweis von Late-Gadolinium-Enhancement

Nach der Standard-Referenz-Sequenz hatten 201 (67,4%) Patienten einen positiven LGE Befund, davon 143 mit KHK, 31 mit HCM und 27 mit inflammatorischer Herzerkrankung. Alle 201 positiven Befunde wurden ebenfalls mittels bSSFP-IR gesehen. Mit beiden bSSFP-PSIR Aufnahmen wurden zwei kleine Narben (<1g) bei einem Patienten mit Infarkt und einem Patienten mit HCM übersehen.[2]
In der quantitativen LGE-Analyse wurde kein signifikanter Unterschied in der mittleren Narbengröße zwischen der Standard-Referenz-Sequenz und den Multislice-Sequenzen gefunden. [2]
Atemanhalte bzw. freie Atmung hatten keine Einfluss auf die Narbengröße (s. Tabelle 3). [2]

	Alle Gruppen	KHK	HCM	Inflammatorische Herzerkrankung	
FLASH-PSIR	8,96 ± 10,64 g	7,46 ± 6,65 g	15,42 ± 20,00 g	9,39 ± 10,28 g	
SSFP-IR	8,69 ± 10,75 g	7,26 ± 7,03 g	15,31 ± 20,02 g	8,67 ± 9,66 g	p > 0.05
SSFP-PSIR	9,05 ± 10,84 g	7,68 ± 7,18 g	15,51 ± 20,31 g	8,89 ± 9,30 g	p > 0.05
SSFP-PSIR freie Atmung	8,85 ± 10,71 g	7,41 ± 6,91g	15,38 ± 19,96 g	8,97 ± 9,94 g	p > 0.05

Die Werte zeigen die mittlere LGE Größe in Gramm. P Werte für jede Multislice-Sequenz verglichen mit FLASH-PSIR in allen Gruppen

Tabelle 3 Quantitative Auswertung der LGE-Größe (übersetzt aus [2])

Bei Patienten mit Arrhythmien wurde die Standard-Referenz-Sequenz nicht ausgewertet, da der Anteil der nicht-diagnostischen Bilder zu hoch war. Die Auswertung der Multislice-Sequenzen war möglich. Die mittlere Narbengröße unterschied sich nicht signifikant.[2]

3.3. Gewebedifferenzierung zur Vorhersage einer Anthrazyklin-induzierten Kardiomyopathie

Von den anfangs 30 eingeschlossenen Patienten mussten im Verlauf sieben Patienten ausgeschlossen werden, da sie die Studie vorzeitig abbrachen (n=2 Patientenwunsch, n=5 vorzeitige Beendigung der Chemotherapie), so dass 23 Patienten analysiert werden konnten.[3]

3.3.1 Einfluss der Anthrazyklintherapie auf die kardiale Funktion

Am Ende der Studie hatten neun Patienten eine LV-EF Reduktion um > 10% entwickelt und entsprachen damit der Definition der aKMP. Diese Patientengruppe hatte zu Beginn der Studie eine mittlere LV-EF von 63,5% ± 5,8% und eine mittlere LV-EF von 49,9% ± 5,0% nach Chemotherapie (p<0,01). Bei den übrigen Patienten änderte sich die LV-EF nicht signifikant (zu Beginn der Studie 59,2% ± 10,3%, nach Chemotherapie 58,3% ± 7,8% (p=0,47)) (s. Abbildung 3). [3]

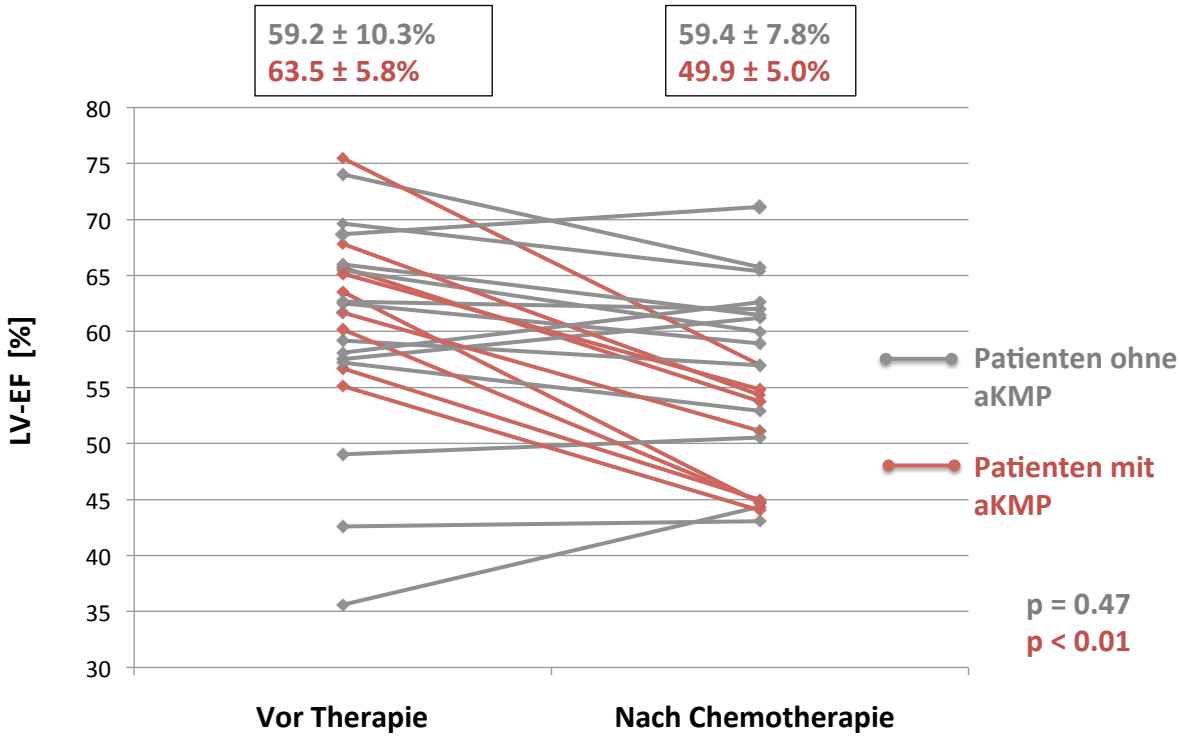

Abbildung 3 Entwicklung der linksventrikulären Ejektionsfraktion (LV-EF) vor und nach der Chemotherapie. Die roten Punkte/Linien zeigen Patienten, die eine anthrazyklin-induzierte Kardiomyopathie (aKMP) definiert als einen Abfall von >10% der LV-EF entwickelt haben. Die durchschnittliche LV-EF für Patienten mit und ohne aKMP sind oberhalb der Abbildung dargestellt. (übersetzt aus [3])

Ebenso reduzierte sich die LV-Masse in der Gruppe der aKMP-Patienten signifikant (zu Beginn der Studie 86,9 ± 24,5 g, nach Chemotherapie 81,1 ± 22,3 g (p= 0,002)), die LV-Masse der übrigen Patienten änderte sich nicht signifikant (zu Beginn der Studie 81,8 ± 21,0 g, nach Chemotherapie 79,2 ± 18,1 g).[3]

Bei den Patienten, die keine aKMP im Verlauf entwickelten, erhöhten sich jedoch die LV-EF und das LV-EDV sowie die RV-EF innerhalb der ersten 48 Stunden nach Beginn der Therapie signifikant (LV-EF: 59,2 % ± 10,2% vs. 63,9% ± 7,9% (p= 0,02); LV-EDV: 165,1 ± 39,6 vs. 177,5 ± 36,2 ml (p=0,03); RV-EF: 47,3% ± 5,9% vs. 52,1% ± 6,2% (p<0,01)). [3]

3.3.2 Einfluss der Anthrazyklintherapie auf das kardiale Gewebe

3.3.2.1 Parametrisches T1-Mapping

Die Patienten, die eine aKMP entwickelten, zeigten einen signifikanten Abfall der

nativen T1 Zeit von 1002,0 ± 37,9 ms zu Beginn der Therapie auf 956,5 ± 29,2 ms 48 Stunden nach Erstgabe des Medikaments ($p<0,01$). Patienten, die keine aKMP entwickelten, zeigten diesen signifikanten Abfall nicht (T1 Zeit zu Beginn der Therapie 990,9 ± 56,4 ms vs. 978,4 ± 57,4 ms nach 48 Stunden ($p=0,08$)).[3]

Nach Beendigung der Chemotherapie unterschieden sich die T1 Zeiten weder bei den Patienten ohne aKMP noch bei den Patienten mit aKMP von den T1 Zeiten zu Beginn der Studie (s. Abbildung 4).[3]

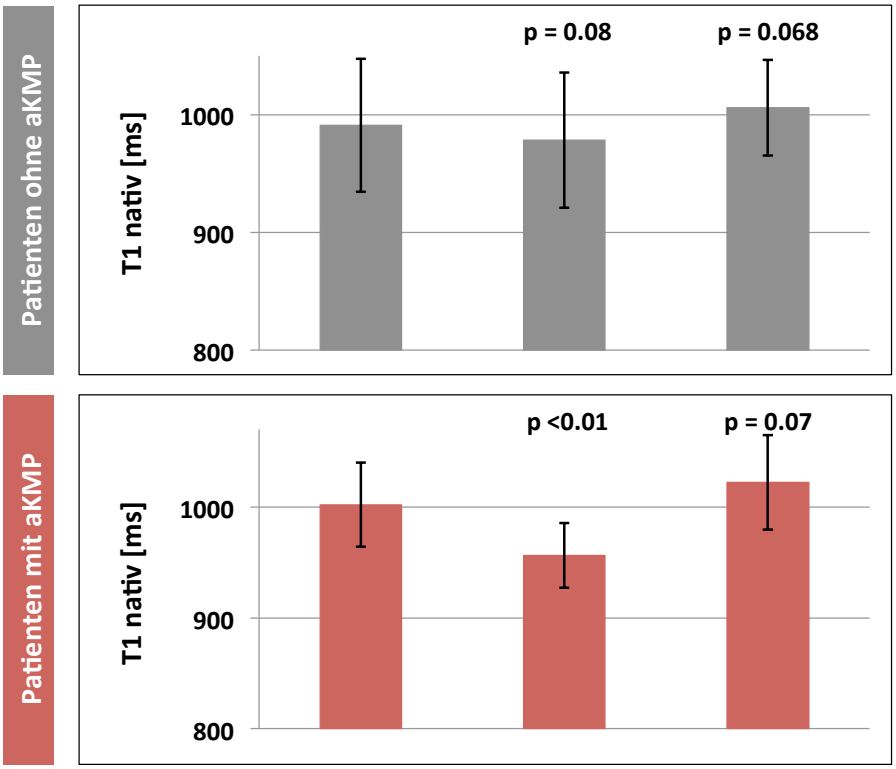

Abbildung 4 Natives T1 Mapping. Die grauen Balken repräsentieren die Patienten, die keine anthrazyklin-induzierte Kardiomyopathie (aKMP) entwickelt haben, die roten Balken die Patienten mit aKMP. P Werte zeigen statistische Signifikanzen im Vergleich zu den T1 Zeiten der Erstuntersuchung (vor Beginn der Therapie). (übersetzt aus [3])

3.3.2.2 Late-Gadolinium-Enhancement

Die Analyse des LGE zeigte bei drei Patienten bereits zu Beginn der Studie Fibrose. Einer dieser Patienten entwickelte im Verlauf der Studie eine aKMP, die zwei anderen entwickelten keine aKMP, hatten aber eine vorab bekannte KHK. Die Läsionen veränderten sich nicht im Verlauf der Studie. Sie entwickelten auch keine

neuen Läsionen. Ebenso entwickelte kein anderer Patient im Verlauf der Studie eine Läsion.[3]

4. Diskussion

Die dissertationsrelevanten Studien zeigen eine zeiteffizientere Anwendung der kardiovaskulären MRT für eine breitere Anwendung in der klinischen Routine für eine Erleichterung der Nutzung ihrer diagnostischen Möglichkeiten und zeigen neue Nutzungsmöglichkeiten auf [1-3].

Eine Möglichkeit zur zeiteffizienteren Anwendung der kardiovaskulären MRT ist die Nutzung bereits vorhandener Routineaufnahmen zur Erweiterung der Auswertung. Für diese Möglichkeit ist die Etablierung von Normwerten basierend auf Routineaufnahmen notwendig. Wir erstellten Normwerte für Volumina und Funktion des LA basierend auf Routineaufnahmen zur LV-Funktionsauswertung [1]. Hierdurch wird eine valide Einschätzung des LA ohne zusätzliche Aufnahmezeit ermöglicht.
Die Evaluation des LA kann grundsätzlich entweder biplan oder mittels mehrerer kurzer Achsen dreidimensional erfolgen. Beide Möglichkeiten sind genau [22], so dass die biplane Auswertung auf Basis der bereits routinemäßig vorhandenen langen Achsen die zeiteffizientere Möglichkeit darstellt.
Als Auswerteparameter kann die Fläche und/oder das Volumen angegeben werden [12, 14, 15].Es wurde allerdings gezeigt, dass Volumina ein besserer Prädiktor für kardiovaskuläre Ereignisse sind [23].
Wir erstellten Normwerte für Volumina und Funktion des linken Vorhofs abhängig von Alter, Geschlecht und Feldstärke [1]. Dabei konnten wir eine Abnahme des LA-EDV mit zunehmendem Alter darstellen, was auch bereits in einigen vorherigen Studien gezeigt wurde [11, 12]. In anderen Studien konnte dies nicht gezeigt werden [14, 24], in diesen Studien wurden jedoch Probanden über 50 Jahren mit Probanden unter 50 Jahren verglichen. Wir konnten zeigen, dass die Veränderung bereits früher stattfindet [1].
Wie auch bereits bei Hudsmith et al. fanden wir signifikante Unterschiede zwischen den Geschlechtern [1, 13], welche jedoch nach Normierung auf Körpergröße oder BSA nicht mehr zu sehen waren [1].

Dieses Ergebnis unterstützt die Bedeutung der Normierung kardialer Werte, um Fehleinschätzungen zu vermeiden.

Eine Abhängigkeit der Werte von der Feldstärke gab es nicht [1]. Dies deckt sich mit der Erfahrung der Evaluation der linksventrikulären Volumina und Funktion, die ebenfalls auf SSFP cine Bildern beruht [25].

Die Quantifizierung der LA-EF sowie der Volumina wird aktuell noch nicht flächendeckend in eine Routine-Untersuchung einbezogen. Dies liegt auch an der bisherigen Annahme, dass hierfür zusätzliche, zeitkostende Aufnahmen notwendig seien. Allerdings gelangt die Bedeutsamkeit der LA-EF als Indikator für kardiale Veränderungen und Prognosen immer mehr in das Bewusstsein. Eine erniedrigte LA-EF findet sich sowohl bei systolischer und diastolischer Herzinsuffizienz [26] als auch bei Herzinsuffizienz mit erhaltener LV-EF [27]. Durch die von uns ermittelten Normwerte auf Basis des zeitsparenden Routineprotokolls kann die Untersuchung um diese Information ergänzt werden, ohne hierbei zusätzliche Zeit zu benötigen [1].

4.1 Etablierung zeitsparender Late-Gadolinium-Enhancement Sequenzen

Die Einführung neuer Techniken, insbesondere der Multislice-Technik, kann ebenfalls die Untersuchungsdauer verkürzen.

In unserer Studie konnten wir zeigen, dass zwei neu entwickelte Multislice LGE-Sequenzen als mindestens gleichwertig zu der Standard-LGE-Sequenz zu betrachten sind. Die visuelle und quantitative Narbenerkennung unterschied sich nicht signifikant.[2]

Die Aufnahmedauer der Multislice-Sequenzen war deutlich kürzer als die der Standard-Sequenz. Zusätzlich konnten diese Sequenzen auch noch qualitativ ausreichende Bilder bei Patienten mit Arrhythmien und/oder Schwierigkeiten, den Atem anzuhalten, liefern und eigneten sich damit besser für schwerkranke Patienten. Diese Überlegenheit der Multislice-Aufnahmen konnten auch schon in anderen Studien gezeigt werden [28, 29].

Allerdings wurden bei zwei Patienten sehr kleine LGE Läsionen mit der multislice bSSFP-PSIR übersehen, die in der Standard-Referenzsequenz und in der bSSFP-IR Sequenz gesehen wurden. Die Läsionen betrugen jedoch je weniger als ein Gramm. Eine mögliche Erklärung wäre, dass Partialvolumeneffekte oder eine veränderte

Schichtposition auf Grund stärkerer Atembewegungen dazu beigetragen haben. Dennoch ist nicht sicher auszuschließen, dass sehr kleine Läsionen durch die bSSFP-PSIR Sequenz übersehen werden können.[2]
Da jedoch auch bereits kleine Läsionen einen prognostischen Wert für Patienten mit Kardiomyopathien haben [30-33] und bei inflammatorischen Herzerkrankungen sogar die Diagnose beeinflussen können [34], sollten bei Fragestellungen nach HCM, inflammatorischer Herzerkrankung oder zur Differenzierung einer Kardiomyopathie segmentierte FLASH-PSIR Aufnahmen durchgeführt werden solange ein stabiler Sinusrhythmus vorliegt und der Patient den Atem anhalten kann. [2]
Aktuell gibt es weiterhin Bestrebungen, die Sequenzen zur LGE-Darstellung insbesondere auch für Patienten mit Arrhythmien und Atemanhalteschwierigkeiten weiter zu verbessern. Hierzu zählt auch die bewegungskorrigierte (motion corrected = MOCO) bSSFP-PSIR Sequenz, die eine deutliche Verbesserung der Bildqualität der LGE-Aufnahmen insbesondere bei diesen Patienten erbringt [35], so dass eine abschließende Empfehlung zur Nutzung der LGE- Sequenzen noch nicht gegeben werden kann.

4.2 Klinische Anwendbarkeit und diagnostischer Wert der Gewebedifferenzierung

Durch diese neuen Multislice-LGE-Techniken besteht eine Möglichkeit zur zeitsparenderen Gewebedifferenzierung.
Neben der Narbendarstellung kann mittels kardiovaskulärer MRT das myokardiale Gewebe jedoch noch weiter differenziert werden. Hierzu zählt das parametrische T1 Mapping. Dieses ist nicht nur ein Marker für diffuse Fibrose bei chronischen Prozessen [36-38], es zeigt auch bereits Gewebeveränderungen im akuten Stadium an [39, 40].
In unserer Studie zur Gewebedifferenzierung des Myokards bei aKMP konnten wir zeigen, dass Sarkompatienten, die nach 6 Monaten Therapie mit Anthrazyklinen eine aKMP entwickelten, bereits 48 Stunden nach Therapiebeginn erniedrigte Werte im T1 Mapping aufwiesen. Bei denjenigen, die keine aKMP entwickelten, wurde dieser Abfall nicht gesehen. Nach 6 Monaten hatte sich die T1 Zeit auch bei den Patienten mit aKMP wieder erholt. Dadurch liegt die Vermutung nahe, dass es sich in diesem Fall eher um akute toxische Effekte der myokardialen Veränderung als um Langzeiteffekte wie eine interstitielle Fibrose handelt.[3]

Die Prävalenz einer aKMP liegt bei 3% - 48% und ist abhängig von unterschiedlichen Faktoren [19, 41, 42]. Eine frühzeitige Erkennung ist wichtig. Nach aktuellen Guidelines werden die Patienten hierfür engmaschig echokardiographisch kontrolliert, um bei einem Abfall der LV-EF zügig mit der entsprechenden Therapie beginnen zu können [43, 44].
Studien haben bereits die Überlegenheit der kardiovaskulären MRT gegenüber der Echokardiographie bezüglich der LV-EF-Abnahme unter Anthrazyklin-Therapie gezeigt [45]. Jedoch ist die Anwendung der Echokardiographie aktuell aus Praktikabilitätsgründen noch weiter verbreitet. Mit der zusätzlichen Möglichkeit zur Gewebedifferenzierung hat die kardiovaskuläre MRT jedoch ein Alleinstellungsmerkmal.
In anderen Studien wurde die Erhöhung von T1 Zeiten Jahre nach Beendigung der Anthrazyklin-Therapie beobachtet [46, 47]. In unserer Studie hingegen beobachteten wir einen Abfall der T1 Zeit direkt nach Beginn der Anthrazyklin-Therapie. Da dieser nur bei Patienten auftrat, die im Verlauf eine aKMP entwickelten, kann dieser Parameter die gefährdeten Patienten bereits frühzeitig identifizieren. [3]
Insgesamt kann die T1 Zeit ein gutes Hilfsmittel zur Früherkennung der Entwicklung und Risikostratifizierung einer aKMP sein. Im Gegensatz zu anderen bildgebenden Parametern, sowie zum Beispiel der LV-EF, kann sie bereits vor Entwicklung der aKMP detektiert werden und somit möglicherweise die Therapie bereits frühzeitig beeinflussen. [3]

4.3 Zusammenfassung

Die kardiovaskuläre MRT hat in den vergangenen Jahren enorme Fortschritte sowohl in der technischen Durchführbarkeit als auch in den Anwendungsbereichen gemacht. Dennoch ist sie nicht so weit verbreitet, wie ihre diagnostischen Möglichkeiten es anbieten würden. Einer der Hauptgründe für diese Einschränkung ist die Untersuchungsdauer.

Durch die hier vorgelegten dissertationsrelevanten Studien können kardiovaskulären MRT-Untersuchungen zeiteffizienter durchgeführt werden. Einerseits gehört dazu die Ausdehnung der Nutzung bereits akquirierter Routineaufnahmen. Hierzu erstellten wir Normwerte für die linksatriale Funktion auf Basis der Routineaufnahmen für die linksventrikuläre Funktion. Andererseits gehört dazu die Etablierung zeitsparenderer

Techniken, wobei wir eine zeitsparende Multislice-Technik zur Gewebedifferenzierung etablierten. Die Notwendigkeit der nicht-invasiven Gewebedifferenzierung – dem Alleinstellungsmerkmal der kardiovaskulären MRT – konnten wir in unserer Studie zur frühzeitigen Erkennung einer anthrazyklin-induzierten Kardiomyopathie zeigen.

Insgesamt werden diese Studien helfen, die Akzeptanz und damit Verbreitung und Anwendung der kardiovaskulären MRT weiter voranzubringen.

5. Literaturverzeichnis

1. Funk S, Kermer J, Doganguezel S, Schwenke C, von Knobelsdorff-Brenkenhoff F, Schulz-Menger J. Quantification of the left atrium applying cardiovascular magnetic resonance in clinical routine. Scand Cardiovasc J. 2018;52(2):85-92.
2. Muehlberg F, Arnhold K, Fritschi S, Funk S, Prothmann M, Kermer J, Zange L, von Knobelsdorff-Brenkenhoff F, Schulz-Menger J. Comparison of fast multi-slice and standard segmented techniques for detection of late gadolinium enhancement in ischemic and non-ischemic cardiomyopathy - a prospective clinical cardiovascular magnetic resonance trial. J Cardiovasc Magn Reson. 2018;20(1):13.
3. Muehlberg F, Funk S, Zange L, von Knobelsdorff-Brenkenhoff F, Blaszczyk E, Schulz A, Ghani S, Reichardt A, Reichardt P, Schulz-Menger J. Native myocardial T1 time can predict development of subsequent anthracycline-induced cardiomyopathy. ESC Heart Fail. 2018.
4. von Knobelsdorff-Brenkenhoff F, Pilz G, Schulz-Menger J. Representation of cardiovascular magnetic resonance in the AHA / ACC guidelines. J Cardiovasc Magn Reson. 2017;19(1):70.
5. von Knobelsdorff-Brenkenhoff F, Schulz-Menger J. Role of cardiovascular magnetic resonance in the guidelines of the European Society of Cardiology. J Cardiovasc Magn Reson. 2016;18:6.
6. Ahmed S, Shellock FG. Magnetic resonance imaging safety: implications for cardiovascular patients. J Cardiovasc Magn Reson. 2001;3(3):171-82.
7. Pennell DJ. Cardiovascular magnetic resonance: twenty-first century solutions in cardiology. Clin Med (Lond). 2003;3(3):273-8.
8. Grothues F, Smith GC, Moon JC, Bellenger NG, Collins P, Klein HU, Pennell DJ. Comparison of interstudy reproducibility of cardiovascular magnetic resonance with two-dimensional echocardiography in normal subjects and in patients with heart failure or left ventricular hypertrophy. Am J Cardiol. 2002;90(1):29-34.
9. Greenwood JP, Maredia N, Younger JF, Brown JM, Nixon J, Everett CC, Bijsterveld P, Ridgway JP, Radjenovic A, Dickinson CJ, Ball SG, Plein S. Cardiovascular magnetic resonance and single-photon emission computed tomography for diagnosis of coronary heart disease (CE-MARC): a prospective trial. Lancet. 2012;379(9814):453-60.
10. Friedrich MG, Sechtem U, Schulz-Menger J, Holmvang G, Alakija P, Cooper LT, White JA, Abdel-Aty H, Gutberlet M, Prasad S, Aletras A, Laissy JP, Paterson I, Filipchuk NG, Kumar A, Pauschinger M, Liu P. Cardiovascular magnetic resonance in myocarditis: A JACC White Paper. J Am Coll Cardiol. 2009;53(17):1475-87.
11. Maceira AM, Cosin-Sales J, Prasad SK, Pennell DJ. Characterization of left and right atrial function in healthy volunteers by cardiovascular magnetic resonance. J Cardiovasc Magn Reson. 2016;18(1):64.
12. Maceira AM, Cosin-Sales J, Roughton M, Prasad SK, Pennell DJ. Reference left atrial dimensions and volumes by steady state free precession cardiovascular magnetic resonance. J Cardiovasc Magn Reson. 2010;12:65.
13. Hudsmith LE, Petersen SE, Francis JM, Robson MD, Neubauer S. Normal human left and right ventricular and left atrial dimensions using steady state free precession magnetic resonance imaging. J Cardiovasc Magn Reson. 2005;7(5):775-82.
14. Sievers B, Kirchberg S, Franken U, Bakan A, Addo M, John-Puthenveettil B, Trappe HJ. Determination of normal gender-specific left atrial dimensions by

cardiovascular magnetic resonance imaging. J Cardiovasc Magn Reson. 2005;7(4):677-83.
15. Anderson JL, Horne BD, Pennell DJ. Atrial dimensions in health and left ventricular disease using cardiovascular magnetic resonance. J Cardiovasc Magn Reson. 2005;7(4):671-5.
16. Sievers B, Elliott MD, Hurwitz LM, Albert TS, Klem I, Rehwald WG, Parker MA, Judd RM, Kim RJ. Rapid detection of myocardial infarction by subsecond, free-breathing delayed contrast-enhancement cardiovascular magnetic resonance. Circulation. 2007;115(2):236-44.
17. Nguyen TD, Spincemaille P, Weinsaft JW, Ho BY, Cham MD, Prince MR, Wang Y. A fast navigator-gated 3D sequence for delayed enhancement MRI of the myocardium: comparison with breathhold 2D imaging. J Magn Reson Imaging. 2008;27(4):802-8.
18. Coleman MP, Forman D, Bryant H, Butler J, Rachet B, Maringe C, Nur U, Tracey E, Coory M, Hatcher J, McGahan CE, Turner D, Marrett L, Gjerstorff ML, Johannesen TB, Adolfsson J, Lambe M, Lawrence G, Meechan D, Morris EJ, Middleton R, Steward J, Richards MA. Cancer survival in Australia, Canada, Denmark, Norway, Sweden, and the UK, 1995-2007 (the International Cancer Benchmarking Partnership): an analysis of population-based cancer registry data. Lancet. 2011;377(9760):127-38.
19. Swain SM, Whaley FS, Ewer MS. Congestive heart failure in patients treated with doxorubicin: a retrospective analysis of three trials. Cancer. 2003;97(11):2869-79.
20. Schelbert EB, Fridman Y, Wong TC, Abu Daya H, Piehler KM, Kadakkal A, Miller CA, Ugander M, Maanja M, Kellman P, Shah DJ, Abebe KZ, Simon MA, Quarta G, Senni M, Butler J, Diez J, Redfield MM, Gheorghiade M. Temporal Relation Between Myocardial Fibrosis and Heart Failure With Preserved Ejection Fraction: Association With Baseline Disease Severity and Subsequent Outcome. JAMA Cardiol. 2017;2(9):995-1006.
21. Yingchoncharoen T, Jellis C, Popovic ZB, Wang L, Gai N, Levy WC, Tang WH, Flamm S, Kwon DH. Focal fibrosis and diffuse fibrosis are predictors of reversed left ventricular remodeling in patients with non-ischemic cardiomyopathy. Int J Cardiol. 2016;221:498-504.
22. Childs H, Ma L, Ma M, Clarke J, Cocker M, Green J, Strohm O, Friedrich MG. Comparison of long and short axis quantification of left ventricular volume parameters by cardiovascular magnetic resonance, with ex-vivo validation. J Cardiovasc Magn Reson. 2011;13:40.
23. Tsang TS, Abhayaratna WP, Barnes ME, Miyasaka Y, Gersh BJ, Bailey KR, Cha SS, Seward JB. Prediction of cardiovascular outcomes with left atrial size: is volume superior to area or diameter? J Am Coll Cardiol. 2006;47(5):1018-23.
24. Thomas L, Levett K, Boyd A, Leung DY, Schiller NB, Ross DL. Compensatory changes in atrial volumes with normal aging: is atrial enlargement inevitable? J Am Coll Cardiol. 2002;40(9):1630-5.
25. Hudsmith LE, Petersen SE, Tyler DJ, Francis JM, Cheng AS, Clarke K, Selvanayagam JB, Robson MD, Neubauer S. Determination of cardiac volumes and mass with FLASH and SSFP cine sequences at 1.5 vs. 3 Tesla: a validation study. J Magn Reson Imaging. 2006;24(2):312-8.
26. Pellicori P, Zhang J, Lukaschuk E, Joseph AC, Bourantas CV, Loh H, Bragadeesh T, Clark AL, Cleland JG. Left atrial function measured by cardiac magnetic resonance imaging in patients with heart failure: clinical associations and prognostic value. Eur Heart J. 2015;36(12):733-42.

27. Santos AB, Kraigher-Krainer E, Gupta DK, Claggett B, Zile MR, Pieske B, Voors AA, Lefkowitz M, Bransford T, Shi V, Packer M, McMurray JJ, Shah AM, Solomon SD. Impaired left atrial function in heart failure with preserved ejection fraction. Eur J Heart Fail. 2014;16(10):1096-103.
28. Knowles BR, Caulfield D, Cooklin M, Rinaldi CA, Gill J, Bostock J, Razavi R, Schaeffter T, Rhode KS. 3-D visualization of acute RF ablation lesions using MRI for the simultaneous determination of the patterns of necrosis and edema. IEEE Trans Biomed Eng. 2010;57(6):1467-75.
29. Weingartner S, Akcakaya M, Basha T, Kissinger KV, Goddu B, Berg S, Manning WJ, Nezafat R. Combined saturation/inversion recovery sequences for improved evaluation of scar and diffuse fibrosis in patients with arrhythmia or heart rate variability. Magn Reson Med. 2014;71(3):1024-34.
30. Mikami Y, Cornhill A, Heydari B, Joncas SX, Almehmadi F, Zahrani M, Bokhari M, Stirrat J, Yee R, Merchant N, Lydell CP, Howarth AG, White JA. Objective criteria for septal fibrosis in non-ischemic dilated cardiomyopathy: validation for the prediction of future cardiovascular events. J Cardiovasc Magn Reson. 2016;18(1):82.
31. Lee SA, Yoon YE, Kim JE, Park JJ, Oh IY, Yoon CH, Suh JW, Kim JS, Chun EJ, Cho YS, Youn TJ, Lim C, Cho GY, Chae IH, Park KH, Choi DJ, Choi SI. Long-Term Prognostic Value of Late Gadolinium-Enhanced Magnetic Resonance Imaging in Patients With and Without Left Ventricular Dysfunction Undergoing Coronary Artery Bypass Grafting. Am J Cardiol. 2016;118(11):1647-54.
32. Hulten E, Agarwal V, Cahill M, Cole G, Vita T, Parrish S, Bittencourt MS, Murthy VL, Kwong R, Di Carli MF, Blankstein R. Presence of Late Gadolinium Enhancement by Cardiac Magnetic Resonance Among Patients With Suspected Cardiac Sarcoidosis Is Associated With Adverse Cardiovascular Prognosis: A Systematic Review and Meta-Analysis. Circ Cardiovasc Imaging. 2016;9(9):e005001.
33. Chan RH, Maron BJ, Olivotto I, Pencina MJ, Assenza GE, Haas T, Lesser JR, Gruner C, Crean AM, Rakowski H, Udelson JE, Rowin E, Lombardi M, Cecchi F, Tomberli B, Spirito P, Formisano F, Biagini E, Rapezzi C, De Cecco CN, Autore C, Cook EF, Hong SN, Gibson CM, Manning WJ, Appelbaum E, Maron MS. Prognostic value of quantitative contrast-enhanced cardiovascular magnetic resonance for the evaluation of sudden death risk in patients with hypertrophic cardiomyopathy. Circulation. 2014;130(6):484-95.
34. Grun S, Schumm J, Greulich S, Wagner A, Schneider S, Bruder O, Kispert EM, Hill S, Ong P, Klingel K, Kandolf R, Sechtem U, Mahrholdt H. Long-term follow-up of biopsy-proven viral myocarditis: predictors of mortality and incomplete recovery. J Am Coll Cardiol. 2012;59(18):1604-15.
35. Fan H, Li S, Lu M, Yin G, Yang X, Lan T, Dai L, Chen X, Li J, Zhang Y, Sirajuddin A, Kellman P, Arai AE, Zhao S. Myocardial late gadolinium enhancement: a head-to-head comparison of motion-corrected balanced steady-state free precession with segmented turbo fast low angle shot. Clin Radiol. 2018;73(6):593.e1-.e9.
36. h-Ici DO, Jeuthe S, Al-Wakeel N, Berger F, Kuehne T, Kozerke S, Messroghli DR. T1 mapping in ischaemic heart disease. Eur Heart J Cardiovasc Imaging. 2014;15(6):597-602.
37. Sibley CT, Noureldin RA, Gai N, Nacif MS, Liu S, Turkbey EB, Mudd JO, van der Geest RJ, Lima JA, Halushka MK, Bluemke DA. T1 Mapping in cardiomyopathy at cardiac MR: comparison with endomyocardial biopsy. Radiology. 2012;265(3):724-32.
38. Bull S, White SK, Piechnik SK, Flett AS, Ferreira VM, Loudon M, Francis JM, Karamitsos TD, Prendergast BD, Robson MD, Neubauer S, Moon JC, Myerson SG.

Human non-contrast T1 values and correlation with histology in diffuse fibrosis. Heart. 2013;99(13):932-7.
39. von Knobelsdorff-Brenkenhoff F, Schuler J, Doganguzel S, Dieringer MA, Rudolph A, Greiser A, Kellman P, Schulz-Menger J. Detection and Monitoring of Acute Myocarditis Applying Quantitative Cardiovascular Magnetic Resonance. Circ Cardiovasc Imaging. 2017;10(2).
40. Hinojar R, Foote L, Arroyo Ucar E, Jackson T, Jabbour A, Yu CY, McCrohon J, Higgins DM, Carr-White G, Mayr M, Nagel E, Puntmann VO. Native T1 in discrimination of acute and convalescent stages in patients with clinical diagnosis of myocarditis: a proposed diagnostic algorithm using CMR. JACC Cardiovasc Imaging. 2015;8(1):37-46.
41. Curigliano G, Cardinale D, Dent S, Criscitiello C, Aseyev O, Lenihan D, Cipolla CM. Cardiotoxicity of anticancer treatments: Epidemiology, detection, and management. CA Cancer J Clin. 2016;66(4):309-25.
42. Krischer JP, Epstein S, Cuthbertson DD, Goorin AM, Epstein ML, Lipshultz SE. Clinical cardiotoxicity following anthracycline treatment for childhood cancer: the Pediatric Oncology Group experience. J Clin Oncol. 1997;15(4):1544-52.
43. Tarantini L, Massimo Gulizia M, Di Lenarda A, Maurea N, Giuseppe Abrignani M, Bisceglia I, Bovelli D, De Gennaro L, Del Sindaco D, Macera F, Parrini I, Radini D, Russo G, Beatrice Scardovi A, Inno A. ANMCO/AIOM/AICO Consensus Document on clinical and management pathways of cardio-oncology: executive summary. Eur Heart J Suppl. 2017;19(Suppl D):D370-d9.
44. Plana JC, Galderisi M, Barac A, Ewer MS, Ky B, Scherrer-Crosbie M, Ganame J, Sebag IA, Agler DA, Badano LP, Banchs J, Cardinale D, Carver J, Cerqueira M, DeCara JM, Edvardsen T, Flamm SD, Force T, Griffin BP, Jerusalem G, Liu JE, Magalhaes A, Marwick T, Sanchez LY, Sicari R, Villarraga HR, Lancellotti P. Expert consensus for multimodality imaging evaluation of adult patients during and after cancer therapy: a report from the American Society of Echocardiography and the European Association of Cardiovascular Imaging. Eur Heart J Cardiovasc Imaging. 2014;15(10):1063-93.
45. Nabhan C, Byrtek M, Rai A, Dawson K, Zhou X, Link BK, Friedberg JW, Zelenetz AD, Maurer MJ, Cerhan JR, Flowers CR. Disease characteristics, treatment patterns, prognosis, outcomes and lymphoma-related mortality in elderly follicular lymphoma in the United States. Br J Haematol. 2015;170(1):85-95.
46. Neilan TG, Coelho-Filho OR, Shah RV, Feng JH, Pena-Herrera D, Mandry D, Pierre-Mongeon F, Heydari B, Francis SA, Moslehi J, Kwong RY, Jerosch-Herold M. Myocardial extracellular volume by cardiac magnetic resonance imaging in patients treated with anthracycline-based chemotherapy. Am J Cardiol. 2013;111(5):717-22.
47. Tham EB, Haykowsky MJ, Chow K, Spavor M, Kaneko S, Khoo NS, Pagano JJ, Mackie AS, Thompson RB. Diffuse myocardial fibrosis by T1-mapping in children with subclinical anthracycline cardiotoxicity: relationship to exercise capacity, cumulative dose and remodeling. J Cardiovasc Magn Reson. 2013;15:48.

Eidesstattliche Versicherung

„Ich, Stephanie Wiesemann, versichere an Eides statt durch meine eigenhändige Unterschrift, dass ich die vorgelegte Dissertation mit dem Thema: „Kardiovaskuläre Magnetresonanztomographie in der klinischen Routine - Etablierung zeiteffizienter Ansätze“ selbstständig und ohne nicht offengelegte Hilfe Dritter verfasst und keine anderen als die angegebenen Quellen und Hilfsmittel genutzt habe.

Alle Stellen, die wörtlich oder dem Sinne nach auf Publikationen oder Vorträgen anderer Autoren beruhen, sind als solche in korrekter Zitierung (siehe „Uniform Requirements for Manuscripts (URM)“ des ICMJE -*www.**icmje**.org*) kenntlich gemacht. Die Abschnitte zu Methodik (insbesondere praktische Arbeiten, Laborbestimmungen, statistische Aufarbeitung) und Resultaten (insbesondere Abbildungen, Graphiken und Tabellen) entsprechen den URM (s.o) und werden von mir verantwortet.

Meine Anteile an den ausgewählten Publikationen entsprechen denen, die in der untenstehenden gemeinsamen Erklärung mit dem/der Betreuer/in, angegeben sind.

Sämtliche Publikationen, die aus dieser Dissertation hervorgegangen sind und bei denen ich Autor bin, entsprechen den URM (s.o) und werden von mir mit verantwortet.

Die Bedeutung dieser eidesstattlichen Versicherung und die strafrechtlichen Folgen einer unwahren eidesstattlichen Versicherung (§156,161 des Strafgesetzbuches) sind mir bekannt und bewusst.“

_____

Datum Unterschrift

Anteilserklärung an den erfolgten Publikationen

Stephanie Funk hatte folgenden Anteil an den folgenden Publikationen:

Publikation 1: **Funk S**, Kermer J, Doganguezel S, Schwenke C, von Knobelsdorff-Brenkenhoff F, Schulz-Menger J. Quantification of the left atrium applying cardiovascular magnetic resonance in clinical routine. Scand Cardiovasc J. 2018;52(2):85-92.
Journal Impact Factor 2017: 1.449
Beitrag im Einzelnen:

- Idee der Studie/Fragestellung
- Literaturrecherche
- Konzeption
- Datenzusammmentragung
- Erstellung des Auswerteprozesses (d.h. anhand von Literatur und klinisch-pathophysiologischer Überlegungen Festlegung der Art der Bildauswertung, Ermitteln und Sicherstellen der technischen Auswertemöglichkeiten)
- Etablierung der Auswertemethode, Auswertung und Supervision der weiteren Anwendung
- statistische Auswertung in Kommunikation mit dem Statistiker Dr. Carsten Schwenke und Interpretation der Daten
- Entwurf des Manuskripts, aller Tabellen und Abbildungen
- Diskussion mit den Koautoren
- Revision des Manuskripts, der Tabellen und Abbildungen

Publikation 2: Muehlberg F, Arnhold K, Fritschi S, **Funk S**, Prothmann M, Kermer J, Zange L, von Knobelsdorff-Brenkenhoff F, Schulz-Menger J. Comparison of fast multi-slice and standard segmented techniques for detection of late gadolinium enhancement in ischemic and non-ischemic cardiomyopathy - a prospective clinical cardiovascular magnetic resonance trial. J Cardiovasc Magn Reson. 2018;20(1):13.
Journal Impact Factor 2017: 5.457
Beitrag im Einzelnen:

- Einschluss/Aufklärung von Patienten (teilweise, ca. 40%)
- Beteiligung an der Datenakquise

- Auswertung eines Teils der Daten - Interobserveranalyse
- Ko-erstellung des Manuskripts und Beteiligung an der Revision, der Tabellen und Abbildungen

Publikation 3: Muehlberg F, **Funk S**, Zange L, von Knobelsdorff-Brenkenhoff F, Blaszczyk E, Schulz A, Ghani S, Reichardt A, Reichardt P, Schulz-Menger J. Native myocardial T1 time can predict development of subsequent anthracycline-induced cardiomyopathy. ESC Heart Fail. 2018.
Journal Impact Factor: nicht verfügbar
Beitrag im Einzelnen:

- Unterstützung bei der Konzeption
- Teilweise Einschluss/Aufklärung von Patienten (ca. 20%)
- Beteiligung an der Datenakquise
- Auswertung eines Teils der Daten (Interobserveranalyse)
- Unterstützung bei Interpretation und Diskussion der Daten
- Ko-erstellung des Manuskripts und Beteiligung an der Revision, der Tabellen und Abbildungen

_____

Unterschrift, Datum und Stempel des betreuenden Hochschullehrers/der betreuenden Hochschullehrerin

_____

Unterschrift des Doktoranden/der Doktorandin

Quantification of the left atrium applying cardiovascular magnetic resonance in clinical routine.

Funk S, Kermer J, Doganguezel S, Schwenke C, von Knobelsdorff-Brenkenhoff F, Schulz-Menger J

Scand Cardiovasc J. 2018 Apr;52(2):85-92. doi: 10.1080/14017431.2017.1423107

https://doi.org/10.1080/14017431.2017.1423107

Muehlberg et al. Journal of Cardiovascular Magnetic Resonance (2018) 20:13
https://doi.org/10.1186/s12968-018-0434-2

Journal of Cardiovascular Magnetic Resonance

RESEARCH Open Access

Comparison of fast multi-slice and standard segmented techniques for detection of late gadolinium enhancement in ischemic and non-ischemic cardiomyopathy – a prospective clinical cardiovascular magnetic resonance trial

Fabian Muehlberg[1*], Kristin Arnhold[1], Simone Fritschi[1], Stephanie Funk[1], Marcel Prothmann[1], Josephine Kermer[1], Leonora Zange[1], Florian von Knobelsdorff-Brenkenhoff[2] and Jeanette Schulz-Menger[1]

Abstract

Background: Segmented phase-sensitive inversion recovery (PSIR) cardiovascular magnetic resonance (CMR) sequences are reference standard for non-invasive evaluation of myocardial fibrosis using late gadolinium enhancement (LGE). Several multi-slice LGE sequences have been introduced for faster acquisition in patients with arrhythmia and insufficient breathhold capability.
The aim of this study was to assess the accuracy of several multi-slice LGE sequences to detect and quantify myocardial fibrosis in patients with ischemic and non-ischemic myocardial disease.

Methods: Patients with known or suspected LGE due to chronic infarction, inflammatory myocardial disease and hypertrophic cardiomyopathy (HCM) were prospectively recruited. LGE images were acquired 10–20 min after administration of 0.2 mmol/kg gadolinium-based contrast agent. Three different LGE sequences were acquired: a segmented, single-slice/single-breath-hold fast low angle shot PSIR sequence (FLASH-PSIR), a multi-slice balanced steady-state free precession inversion recovery sequence (bSSFP-IR) and a multi-slice bSSFP-PSIR sequence during breathhold and free breathing. Image quality was evaluated with a 4-point scoring system. Contrast-to-noise ratios (CNR) and acquisition time were evaluated. LGE was quantitatively assessed using a semi-automated threshold method. Differences in size of fibrosis were analyzed using Bland-Altman analysis.
(Continued on next page)

* Correspondence: fabian.muehlberg@gmail.com
[1]Working Group on Cardiovascular Magnetic Resonance, Experimental and Clinical Research Center - a joint cooperation between the Charité Medical Faculty and the Max-Delbrück Center for Molecular Medicine and HELIOS Hospital Berlin-Buch, Department of Cardiology and Nephrology, Lindenberger Weg 80, 13125 Berlin, Germany
Full list of author information is available at the end of the article

(Continued from previous page)

Results: Three hundred twelve patients were enrolled ($n = 212$ chronic infarction, $n = 47$ inflammatory myocardial disease, $n = 53$ HCM) Of which 201 patients (67,4%) had detectable LGE ($n = 143$ with chronic infarction, $n = 27$ with inflammatory heart disease and $n = 31$ with HCM). Image quality and CNR were best on multi-slice bSSFP-PSIR. Acquisition times were significantly shorter for all multi-slice sequences (bSSFP-IR: 23.4 ± 7.2 s; bSSFP-PSIR: 21.9 ± 6.4 s) as compared to FLASH-PSIR (361.5 ± 95.33 s). There was no significant difference of mean LGE size for all sequences in all study groups (FLASH-PSIR: 8.96 ± 10.64 g; bSSFP-IR: 8.69 ± 10.75 g; bSSFP-PSIR: 9.05 ± 10.84 g; bSSFP-PSIR free breathing: 8.85 ± 10.71 g, $p > 0.05$).
LGE size was not affected by arrhythmia or absence of breathhold on multi-slice LGE sequences.

Conclusions: Fast multi-slice and standard segmented LGE sequences are equivalent techniques for the assessment of myocardial fibrosis, independent of an ischemic or non-ischemic etiology. Even in patients with arrhythmia and insufficient breathhold capability, multi-slice sequences yield excellent image quality at significantly reduced scan time and may be used as standard LGE approach.

Trial registration: ISRCTN48802295 (retrospectively registered).

Keywords: Cardiac MR, CMR, Late gadolinium enhancement, Single-shot, Hypertrophic cardiomyopathy, Myocardial infarction, Inflammatory heart disease, Myocarditis

Background

Late gadolinium enhancement (LGE) cardiovascular magnetic resonance (CMR) is a well-established method for assessment of focal myocardial fibrosis and scarring in ischemic and non-ischemic cardiomyopathies [1–4]. The presence and extent of LGE has been shown to be associated with worse patient outcome in a variety of diseases, i.e. myocardial infarction, hypertrophic cardiomyopathy (HCM) and acute or chronic inflammatory heart disease [5–7]. Hence, the assessment of LGE is integrated into many clinical guidelines and is an integral part of most contrast-based CMR protocols [8–10].

The reference standard technique for LGE assessment is typically based on phase-sensitive inversion recovery (PSIR) sequences that are acquired in a single-slice, single-breathhold fashion [11, 12]. These segmented PSIR LGE images generate excellent image quality at a high spatial resolution if the individual patient has sufficient breathhold capabilities and is in sinus rhythm [13].

However, with the more widespread use of CMR in clinical routine increasing numbers of patients referred for CMR present with arrhythmias or an inability for sufficient breathhold for CMR scan. In these patients, conservative segmented PSIR LGE sequences sometimes fail to provide satisfactory image quality for accurate assessment.

Furthermore, standard segmented LGE sequences typically require 5 to 10 min of scan time for complete myocardial coverage. There is a need for faster and more efficient imaging in CMR in order to enable a more wide-spread use of CMR in clinical routine as well as in smaller institutions where access to CMR scanners maybe more restricted [14]. CMR also competes with other non-invasive imaging techniques in terms of scan time optimization leading to efforts for faster standardized CMR scan protocols [15].

In order to address these issues, multi-slice LGE sequences have been developed with acquisition of the entire k-space of an individual image slice within one heart cycle [16]. Different approaches utilize navigator-based, free breathing sequencing which works without breathhold but mostly still requires stable heart rhythm for optimal image quality [17].

Several small clinical studies have shown that multi-slice LGE sequences provide similar image quality to standard segmented LGE sequences [18, 19]. However, the vast majority of these studies investigated only patients with a single disease entity, i.e. myocardial infarction or HCM and/or excluded patients with arrhythmia. Hence, these studies are not reflecting clinical reality where the underlying cause of LGE is often not known prior to the CMR scan and sinus rhythm is often unstable or non-existent.

In this prospective study we intended to determine the comparability of standard segmented PSIR LGE imaging with two different multi-slice LGE sequences with and without breathhold in a large number of patients with ischemic and non-ischemic cardiomyopathy, namely chronic myocardial infarction, HCM and inflammatory heart disease. Furthermore, we explicitly did not exclude patients with arrhythmia. We aimed to assess if multi-slice LGE sequences represent a robust alternative for LGE assessment independent of pathophysiologic origin of LGE, heart rhythm and patient breathhold capabilities.

Methods

Study population

312 consecutive patients with known or suspected LGE were prospectively recruited. All patients were referred for clinical LGE assessment using CMR for both, ischemic and non-ischemic cardiomyopathies, based on the

clinical information provided by the referring cardiologist. A total of 212 patients had chronic myocardial infarction, 53 patients had HCM and 47 patients had inflammatory heart disease.

All patients underwent a single CMR scan with three different LGE sequences. Exclusion criteria were contraindications to CMR and severe chronic renal disease with an estimated glomerular filtration rate < 30 ml/min/1.73m^2. All studies were performed in accordance with the local institutional review board and local ethics committee approval.

Image protocol

All CMR studies were performed on a 1.5 Tesla scanner (AvantoFit®, Siemens Healthineers, Erlangen, Germany). Patients were scanned with electrocardiogram (ECG)-triggering in the supine position using 16-channel surface phased array coils.

All imaging protocols included assessment of myocardial function in balanced steady-state free precession (bSSFP) cine sequences and of myocardial morphology by LGE imaging.

bSSFP cine imaging (TE 1.19 ms, TR 33.36 ms, flip angle 55°, retrospective ECG-triggered gating, matrix 192x156mm, FOV 340 mm, slice thickness 6 mm, bandwidth 930 Hz, 30 phases per heart cycle, iPAT GRAPPA acceleration factor 2) was performed in long axis two- and four-chamber view for biplanar assessment of left ventricular (LV) end-diastolic volume (LVEDV), LV mass (LVM) and LV ejection fraction (LVEF). Contours were drawn manually and biplanar anatomical and functional parameters calculated automatically by the post-processing software according to an established in-line biplane ellipsoid model. [20] The standard three-point method was used on short axis localizers to define standardized long axis two-chamber (one point in the LV apex, one point in the anterior and one point in the inferior wall of the lv myocardium in the slice with the maximum LV area) and four-chamber view (one point in the LV apex, one point in the interatrial septum below the aorta and one point into the most lateral corner of the right ventricle (RV) on the short axis localizer with the maximum RV area).

For LGE imaging, a 0.2 mmol/kg intravenous injection of contrast agent was administered into an antecubital vein. In patients with myocardial infarction or HCM assessment gadoteridol (ProHance®, Bracco S.p.A., Milan, Italy) was used. For patient with known or suspected inflammatory heart disease gadopentetate (Magnevist®, Bayer Healthcare, Wayne, New Jersey, USA) was administered due to established normal values for this contrast agent for the early enhancement technique which was clinically assessed in these patients independently from this study [21].

Ten minutes after contrast administration, a segmented IR cine bSSFP inversion time (TI) scouting sequence was performed at a mid-ventricular short axis location to determine optimal TI [22]. TI was adapted to optimally null the signal of the remote myocardium. Two-dimensional LGE images were acquired in short-axis views covering the entire LV myocardium by using three different LGE sequences: i) a segmented, single-slice, single-breathhold 2D FLASH-based phase-sensitive inversion recovery sequence (FLASH-PSIR) which was considered as the reference standard; ii) a multi-slice 2D bSSFP-based inversion recovery sequence (bSSFP-IR); iii) a multi-slice 2D bSSFP-based PSIR sequence (bSSFP-PSIR).

Sequence details are displayed in Table 1.

All LGE sequences were acquired in end-expiratory breathhold while the bSSFP-PSIR sequence was additionally acquired in free breathing. In case of suspected artifacts in the LGE images a second perpendicular slice through the affected region was acquired or read-out of the phase encoding direction was swapped. Segmented and multi-slice LGE images were acquired in random order. Acquisition times and occurrence of arrhythmia during image acquisition were noted for all sequences.

Qualitative and quantitative image analysis

For all post-processing analyses commercially available software was used (CVI42 Release 5.6.2, Circle Cardiovascular Imaging, Calgary, Canada). A blinded reader performed LV function assessment in bSSFP cine long axis slices. For assessment of LVEF endocardial contours were drawn in the end-diastolic and end-systolic phase of two- and four-chamber view. All parameters were automatically calculated after contouring by the post-processing software. Separately, image quality and quantitative LGE assessment were performed in a random and blinded order.

For 30 randomly selected individuals, the same reader and a second experienced reader repeated analyses for assessment of intra- and interobserver variability.

Image quality

Visual assessment of image quality was performed on all LGE sequences for each patient using a previously established 4-point-scale using the following grading: excellent quality, no artifacts (score of 1); good quality, minimal artifacts (score of 2); moderate quality, some artifacts which may impair diagnostic quality (score of 3); poor quality, unacceptable artifacts (score of 4) [19].

Signal intensities were measured in regions of interest (ROIs) that covered areas of contrast-enhanced myocardium, as well as areas of remote non-enhanced myocardium with an additional ROI located outside the patient for calculation of background noise. Signal enhancement was measured as recommended by Simonetti et al. [12].

Table 1 LGE sequence parameters

		FLASH-PSIR	SSFP-IR	SSFP-PSIR
Mode		Segmented	Multi-slice (single shot)	Multi-slice (single shot)
TE	[ms]	5.17	1.06	1.05
Flip Angle		30°	50°	65°
Field of view	[mm]	350–450	350–450	350–450
Matrix	[mm]	192 × 256	154 × 192	144 × 192
Slice thickness	[mm]	7	7	7
Slice gap	[mm]	0	0	0

TE Echo time

In detail, we calculated signal intensities and their standard deviations in ROIs of LGE-positive myocardium, as well as areas of remote myocardium. Contrast was defined as difference between mean signal intensity of both ROIs. Image noise was defined as the standard deviation of the signal intensity in the normal-appearing myocardium ROI. Contrast-to-noise ratios (CNR) were calculated by using these values. Measurement of signal-to-noise ratios (SNR) is limited on PSIR images conventionally because the measurement of background noise is invalid in the reconstructed images [23]. Therefore, we did not perform SNR assessment.

Visual LGE assessment

The distribution area and transmurality of fibrosis was evaluated according to the American Heart Association (AHA) 16-segment model. The distribution area of scar in each segment was scored by the proportion of scar to each segment (0: no LGE, 1: 1–25%, 2: 26–50%, 3: 51–75%, 4: 76–100%).

For each subject, the number of segments with presence or absence of fibrosis and location within the myocardial wall (subendocardial, intramural, subepicardial, transmural) was noted for each LGE sequence as previously described [24].

Quantitative LGE assessment

Quantification of LGE was performed with the established semi-automated signal threshold versus reference mean (STRM) method as published previously by our and other groups [21, 25, 26]. On all LGE images, endocardial and epicardial contours were manually traced and ROIs were defined in hyperenhanced and remote myocardium.

True LGE was defined by myocardial signal intensity plus 6 standard deviations (SD) above that of remote, normal-appearing myocardium within the same slice in patients with myocardial infarction. For subjects with HCM and inflammatory heart disease, plus 3 SDs were defined as true LGE [27].

The automated LGE detection could be manually corrected by the reader for a specific location to exclude obvious artifacts. After segmentation, myocardial and scar tissue mass (in grams) were calculated and compared for each AHA segment in each sequence.

Statistical analysis

All statistical analyses were conducted by using statistical software package SPSS 17.0 (International Business Machines, Armonk, New York, USA). Quantitative data are expressed as means ± SD. Sample size was calculated by using power analysis for two proportions to reach a statistical power of more than 80% to detect differences of 5%, using the assumption of 16 ± 12 g scar tissue for patients with chronic myocardial infarction, and 9 ± 5 g for HCM and inflammatory heart disease which were reported previously by our group [26].

Image quality scores were compared by using the Mann-Whitney U test. Interobserver and intraobserver agreement was assessed by using Cohen k statistics.

Statistical comparison of means of LGE size in each individual multi-slice technique against the segmented reference standard technique was performed by using two-tailed paired t tests and Bland-Altman analysis. Scar tissue percentages per segment, CNR and signal enhancement ratios were assessed using the Wilcoxon signed rank test, as these values did not show normal distribution.

Results

Patient characteristics

In total, 312 patients were recruited. Fourteen of these patients were excluded due to incomplete image acquisition. All remaining 298 patients were successfully scanned using all techniques and were included in subsequent analyses (203 patients with chronic myocardial infarction, 50 patients with HCM and 45 patients with inflammatory heart disease). Patient characteristics are shown in Table 2. Study individuals with inflammatory heart disease were significantly younger than patients in the other groups. HCM patients had an increased LVM index (LVM-I), decreased LVEDV index (LVEDV-I) and a slightly elevated LVEF. Figure 1 shows representative images of LGE short axis slices for each group and each sequence.

Acquisition time

The average scan time was significantly longer for the reference standard sequence (361.5 ± 95.3 s including breaks between slice acquisitions) than for any multi-slice sequence (SSFP-IR: 23.4 ± 7.2 s; SSFP-PSIR: 21.9 ± 6.4 s, $p < 0.01$ of all sequences against reference standard).

Table 2 Patient Characteristics

	Chronic myocardial infarction	HCM	Inflammatory heart disease
Number of patients	203	50	45
Gender [♂ / ♀]	160 / 43 (78% / 22%)	35 / 15 (72% / 28%)	32 / 13 (71% / 29%)
Age [years]	66.2 ± 10.7	62.0 ± 14.5	46.3 ± 15.4 *
BMI [kg/m2]	27.6 ± 4.2	27.9 ± 4.3	25.8 ± 4.8
HR [min-1]	68.1 ± 11.5	69.8 ± 16.2	72.2 ± 12.9
LVEF [%]	52.9 ± 10.7	63.0 ± 10.9 *	52.6 ± 13.3
LVEDV-I [ml/m^2]	82.5 ± 24.3	69.6 ± 22.1 *	90.9 ± 26.9
SV-I [ml/m^2]	41.9 ± 8.7	43.3 ± 12.6	44.8 ± 8.9
LVM-I [g/m^2]	59.3 ± 15.8	89.5 ± 28.4 *	61.9 ± 17.2
SR / Arrhythmia	166 / 37 (82% / 18%)	39 / 11 (78% / 22%)	38 / 7 (84% / 16%)
LGE detected [yes / no]	176 / 27 (87% / 13%)	39 / 11 (78% / 22%)	32 / 13 (71% / 29%)

HCM Hypertrophic cardiomyopathy; *BMI* Body mass index; *HR* Heart rate; *LVEF* Left ventricular ejection fraction; *LVEDV-I* Left ventricular end-diastolic volume index; *SV-I* Stroke volume index; *LVM-I* Left ventricular mass index. *SR* Sinus rhythm. * $p < 0.05$

Image quality assessment

Image quality scores differed significantly between each multi-slice and the reference standard sequence. However, they were not influenced by disease entity or – regarding bSSFP-PSIR sequence – breathhold versus free breathing acquisition. Overall, bSSFP-PSIR images showed the best image quality scores. (Fig. 2).

Arrhythmia had a negative impact on image quality scores on the segmented FLASH-PSIR sequence, resulting in poor or non-diagnostic image quality in 48,8% of all patients. Image quality score was not influenced by arrhythmia in any multi-slice sequence.

Assessment of infarcted-to-remote area CNR is shown in Table 3. Mean infarcted-to-remote myocardium CNR was significantly higher on bSSFP-PSIR than on reference standard sequences ($p < 0.01$), and on bSSFP-IR lower than reference standard ($p < 0.01$). Free breathing acquisition of bSSFP-PSIR slightly decreased mean infarcted-to-remote area CNR as compared to acquisition under breathhold, however, was still superior to reference standard ($p < 0.01$). LGE due to chronic infarction showed significantly higher CNR values in all sequences than LGE due to HCM or inflammatory heart disease ($p < 0.01$).

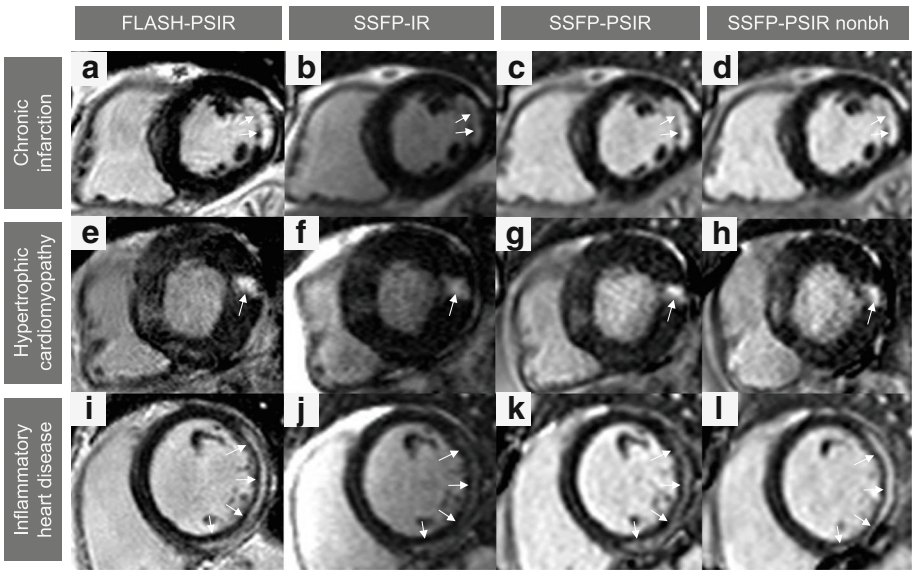

Fig. 1 Representative LGE images. Three selected patients with chronic myocardial infarction (**a**-**d**), hypertrophic cardiomyopathy (**e**-**h**) and acute myocarditis (**i**-**l**) with typical LGE localization: subendocardial for infarction, patchy intramural for HCM and subepicardial for myocarditis. Horizontal rows display corresponding slices of LGE in the same patient, vertical columns show the used techniques: conventional segmented FLASH-PSIR (**a**;**e**;**i**), multi-slice bSSFP-IR (**b**;**f**;**j**), multi-slice bSSFP-PSIR with breathhold (**c**;**g**;**k**) and free-breathing multi-slice bSSFP-IR (**d**;**h**;**l**). nonbh = non-breathhold

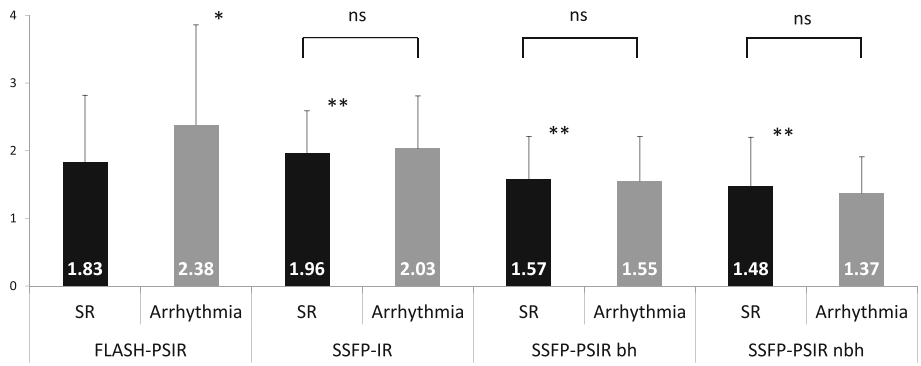

Fig. 2 Image quality scores. Values represent average image quality score for all patients in each group. Score system: 1 = excellent quality, no artifacts; 2 = good quality, minimal artifacts; 3 = moderate quality, some artifacts which may impair diagnostic quality; 4 = poor quality, unacceptable artifacts. * $p < 0.05$ within sequence. ** $p < 0.05$ towards FLASH-PSIR. ns = non-significant, $p > 0.05$. SR = sinus rhythm

Qualitative LGE analysis

Using reference standard sequence, 201 patients (67.4%) had detectable LGE ($n = 143$ with chronic infarction, $n = 31$ with HCM and $n = 27$ with inflammatory heart disease). All 201 LGE-positive patients also had detectable LGE on bSSFP-IR. With both bSSFP-PSIR sequences, two small LGE lesions (< 1 g scar size) were visually not detected in one patient with chronic infarction and one patient with HCM by two blinded readers.

On visual assessment, circumferential extent of scars was similar in all sequences; summation of scores showed excellent matching with reference standard FLASH-PSIR sequence (total score 3875) for bSSFP-PSIR with (total score 3903) and without breathhold (total score 3886) while on bSSFP-IR circumferential scar extent was slightly underestimated (total score 3726). Details are shown in Fig. 3a.

On all multi-slice sequences, the visual allocation of LGE within the myocardial wall (subendocardial, subepicardial, intramural, transmural) showed good matching with FLASH-PSIR for the chronic infarction and inflammatory heart disease group while for inflammatory heart disease there was a higher number of visually transmural LGE areas on bSSFP-PSIR versus FLASH-PSIR (14% versus 10% segments with transmural LGE, see Fig. 3b).

Quantitative LGE analysis

There were no significant differences in mean LGE size between reference standard FLASH-PSIR and multi-slice sequences independent from LGE origin (Table 4). However, Bland-Altman analysis showed that on bSSFP-PSIR LGE size showed a non-significant trend to be smaller in all study groups compared to reference standard - mean difference in LGE size towards reference standard being 0.58 ± 1.99 g on bSSFP-PSIR with breathhold, 0.96 ± 2.03 g on bSSFP-PSIR with free breathing and 0.26 ± 2.4 g on bSSFP-IR (see Fig. 4 for Bland-Altman plots).

The presence or absence of breathhold during LGE imaging using bSSFP-PSIR had no impact on LGE size for any disease entity (Table 4).

Intraobserver agreement (Pearson coefficient) on LGE size was > 0.95 for all sequences. Interobserver agreement was 0.92 for bSSFP-PSIR under free breathing and 0.88 for all other sequences.

In patients with arrhythmia during image acquisition mean LGE size did not differ in any multi-slice sequence, with bSSFP-IR 7.6 ± 6.1 g and bSSFP-PSIR 7.7 ± 5.6 g under breathhold and 7.4 ± 5.6 g under free breathing. Reference standard FLASH-PSIR sequence was not evaluated in arrhythmic patients due to mostly non-diagnostic image quality.

Discussion

The present study compared for the first time a reference standard segmented (FLASH-PSIR) with two multi-slice LGE sequences (bSSFP-IR and bSSFP-PSIR) in 298 patients with ischemic and non-ischemic cardiomyopathies.

Table 3 Contrast-to-noise ratios

	All groups	Chronic infarction	HCM	Inflammatory heart disease
FLASH-PSIR	65.9 ± 71.9	67.9 ± 58.5 *	80.4 ± 126.8	37.0 ± 21.3 *
SSFP-IR	40.1 ± 26.8†	43.2 ± 28.4 *†	38.5 ± 19.9 †	31.5 ± 22.2†
SSFP-PSIR	137.8 ± 103.7†	149.8 ± 114.9 *†	118.4 ± 66.9†	95.7 ± 49.2 *†
SSFP-PSIR nonbh	125.9 ± 72.5†	134.5 ± 72.5 *†	101.7 ± 65.8†	109.0 ± 73.4 †

*p < 0.05 towards the other disease entities for the individual LGE sequence. † p < 0.05 towards FLASH-PSIR gold standard for individual disease entity

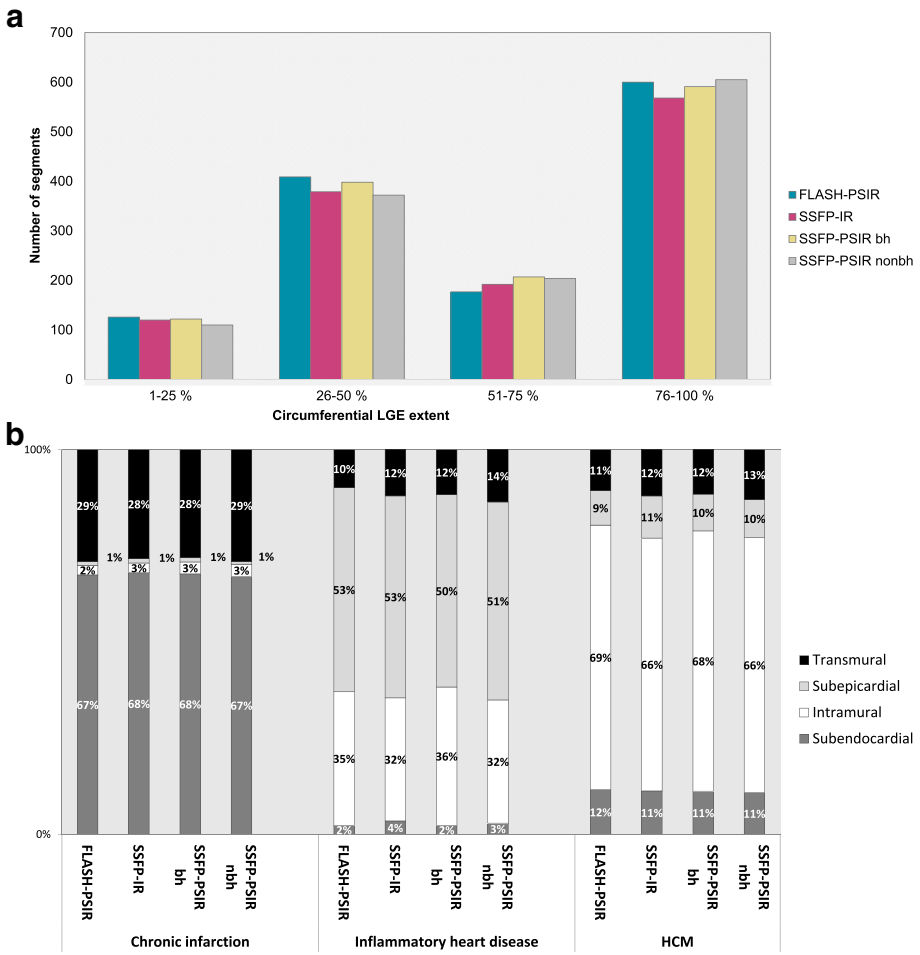

Fig. 3 Visual assessment of LGE. **a**: Visual assessment of circumferential LGE extent. Columns represent number of segments with LGE for different circumferential extents across all study groups (chronic myocardial infarctions, HCM, inflammatory heart disease). **b**: Visual assessment of in-wall LGE location

Our key findings were: Firstly, image quality and CNR were highest on multi-slice bSSFP-PSIR with and without breathhold. Secondly, acquisition time is relevantly shorter on any multi-slice sequence compared to reference standard. Thirdly, visual detection of LGE and visual assessment of LGE extent was consistently very good and equivalent in all sequences. Fourthly, quantification showed no significant difference in LGE size for any multi-slice sequence. Fifthly, in patients with arrhythmia all multi-slice sequences generated good image quality and consistent LGE quantification results, whereas the reference standard provided non-diagnostic image quality in half of all exams. Finally, acquisition of bSSFP-PSIR under free breathing or under breathhold had no impact on LGE detection and quantification. Results were independent of the cause of LGE from ischemic or non-ischemic etiology.

The assessment of myocardial fibrosis has enormous diagnostic and prognostic impact in ischemic and non-ischemic cardiomyopathy [5–7]. Over the last decade

Table 4 Quantitative Assessment - LGE size

	All groups	Chronic infarction	HCM	Inflammatory heart disease	
FLASH-PSIR	8.96 ± 10.64 g	7.47 ± 6.65 g	15.42 ± 20.00 g	9.39 ± 10.28 g	
SSFP-IR	8.69 ± 10.75 g	7.26 ± 7.03 g	15.31 ± 20.02 g	8.67 ± 9.66 g	p > 0.05
SSFP-PSIR	9.05 ± 10.84 g	7.68 ± 7.18 g	15.51 ± 20.31 g	8.89 ± 9.30 g	p > 0.05
SSFP-PSIR nonbh	8.85 ± 10.71 g	7.41 ± 6.91 g	15.38 ± 19.96 g	8.97 ± 9.94 g	p > 0.05

Values represent mean LGE size in gram. *P* values for each multi-slice sequence compared to FLASH-PSIR in all study groups

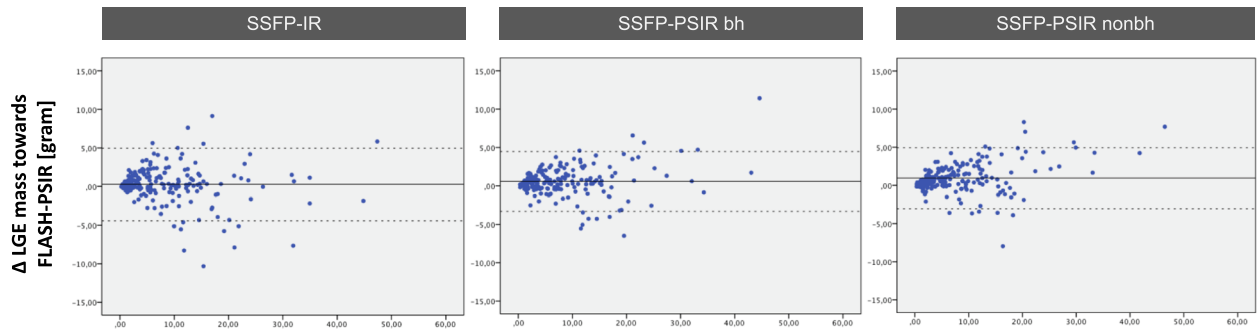

Fig. 4 Bland-Altman plots of LGE mass. Blue dots represent mean LGE size (x-axis) versus delta LGE mass towards FLASH-PSIR (y-axis) in gram for each LGE sequence

many clinical studies have paved the way for CMR to be integrated into a variety of cardiologic, radiologic and other clinical guidelines [9]. The role of LGE in detection of myocardial fibrosis remains unequivocally important despite the development of new parametric mapping techniques, which play an increasing role especially in detection of diffuse fibrosis [28, 29].

Our study demonstrates that bSSFP-PSIR and bSSFP-IR multi-slice LGE sequences provide excellent alternatives to segmented FLASH-PSIR in routine CMR protocols. We showed that not only for ischemic LGE lesions but also for more diffuse lesions in inflammatory heart disease or HCM multi-slice sequences are sufficient to visualize fibrosis and – when quantified in size – show equivalent results compared to the reference standard. The equivalence of multi-slice LGE sequences to segmented sequences has previously been shown in studies for either HCM, ischemic or inflammatory heart disease [18, 19, 30]. However, these studies each used different sequences, smaller patient groups and mostly looked at single disease entities.

The superiority of multi-slice over segmented PSIR sequences in regard to image quality and CNR is in line with other publications [18, 19]. This is attributable to the reduction of motion artifacts and artifacts due to arrhythmia. CNR also depends on the amount of gadolinium-based contrast media in the myocardium, which is influenced by amount and molarity of contrast agent, distribution volume and hemodynamics. As we strictly dosed gadolinium to body weight and tested sequences in a random order, effects on results should be neglectable.

We have also seen variations in CNR between the different disease entities. Since CNR is dependent on the voxel composition of fibrotic tissue, LGE in chronic infarction with more compact fibrosis is expected to result in higher CNR values than LGE in more diffusely fibrotic tissue such as in HCM and inflammatory heart disease.

On bSSFP-PSIR sequence visual assessment revealed slightly larger scar transmurality as compared to the reference standard. We believe that visual assessment of bSSFP-PSIR images is impacted by its comparably higher CNR values which may lead to subjectively higher transmurality of scars.

In two patients, small LGE lesions detectable with the reference standard sequence, were not detected with multi-slice bSSFP-PSIR but, nevertheless, could be visualized with bSSFP-IR. Note that for these two patients LGE amount was less than one gram, which suggests that partial volume effects or shifted slice position due to heavy respiratory motion may have caused the missed lesion. However, it cannot be safely excluded that very small LGE lesions may be missed with multi-slice bSSFP-PSIR due to its different matrix size as compared to the reference standard.

It has been shown that even a small amount of LGE has prognostic implications in cardiomyopathies [31–34]. In case of inflammatory heart disease missed small subepicardial LGE may even impact diagnosis [35], as Lake Louise criteria define myocarditis as two out of three parameters, LGE being one of them [36].

Our results suggest that in patients with known or suspected myocardial infarction bSSFP-PSIR or bSSFP-IR multi-slice sequences can be primarily utilized for LGE detection. In case of an unknown cardiomyopathy or for assessment of HCM and inflammatory heart disease segmented FLASH-PSIR images should be used in scenarios of stable sinus rhythm and sufficient breathhold capabilities. For patients with arrhythmia and/or insufficient breathhold capabilities at the time of CMR scan we showed that segmented sequences fail to provide sufficient image quality. This is in line with previous studies [37, 38]. In these patients we suggest to primarily use multi-slice sequences such as bSSFP-PSIR and/or bSSFP-IR.

In this study two different contrast media were used; gadoteridol in CAD and HCM patients and

gadopentate for inflammatory heart disease. The reason for use of gadopentate was established normal values for relative enhancement sequences, which were acquired in these patients independently from this study. However, there is good evidence that relaxivity and contrast enhancement are nearly identical for both agents so that impact on results should be neglectable. [39]

In our study we explicitly did not exclude patients with arrhythmia. We demonstrated good to excellent image quality and equivalent amount of LGE quantification with all multi-slice sequences. There is no gold standard for LGE detection and quantification in arrhythmic patients. Hence, we cannot definitely state that results are perfectly correct using multi-slice sequences. Still, due to the consistently high image quality scores and – as compared to patients with sinus rhythm – similar CNR values we feel confident that usage of any multi-slice sequence is superior to attempts of segmented image acquisition and shortens scan protocols significantly in these patients.

Interestingly, presence or absence of breathhold during image acquisition on bSSFP-PSIR did not affect detection or quantification of LGE across all study groups. While there must be minimal slice shifting due to respiratory motion on acquisition of an entire LV short axis package within approximately 20 s of acquisition time we could show in a large number of patients that this has no statistically significant effect on diagnostic value. Lower numbers of breathhold cycles may also positively affect patient comfort and may be considered in all patients when SSFP-PSIR sequence is used.

Alternative methods for LGE assessment include 3D sequences, which have been shown to also accurately visualize fibrosis and scarring [40, 41]. These 3D sequences have the advantage of potentially higher spatial resolution, especially in the vertical axis, and the possibility of free movement through the ventricular myocardium. On the other hand, 3D sequences typically require a relatively long acquisition time. This necessitates a continuous adaptation of the optimal myocardial inversion time, which may impair image quality and CNR. Implementation of 3D LGE sequences with dynamic inversion time adjustments may help to overcome this obstacle [42].

In another recent study dark blood PSIR imaging was published using T2 preparation pulses for improved visualization of fibrosis close to the adjacent LV blood pool in 30 patients with subendocardial infarction [43]. This promising technique also included motion correction for acquisition under free breathing but needs to be validated across myocardial disease entities in larger studies.

Conclusions

LGE sequences are a mandatory part of most CMR protocols in ischemic and non-ischemic cardiomyopathy [8]. The broader spread of CMR in clinical routine has several implications: demand for CMR access increases and there is a continuous need for fast scanning protocols [14]. While segmented LGE sequences may give excellent image quality under stable sinus rhythm and sufficient breathhold the issue of time investment prevails. We demonstrated equivalence of multi-slice LGE sequences (bSSFP-IR and bSSFP-PSIR) and segmented FLASH-PSIR sequence in a large number of patients with ischemic and non-ischemic cardiac disease.

For that reason we suggest further strengthening the role of multi-slice sequences in routine CMR protocols whenever it is reliable to use.

Limitations

In spite of the large patient number in this study, all patients were scanned and analyzed in a single CMR center. Male gender was overrepresented in all study groups. Comparability of LGE sequences maybe impacted by different matrix size and, hence, different in-plane resolution used for each sequence. This may also affect SNR and CNR as well as assessment of LGE-positive areas.

Abbreviations

2D: Two-dimensional; AHA: American Heart Association; BMI: Body mass index; bSSFP: Balanced steady-state free precession; CMR: Cardiovascular magnetic resonance; CNR: Contrast-to-noise ratio; FLASH: Fast low angle shot; HCM: Hypertrophic cardiomyopathy; HR: Heart rate; IR: Inversion recovery; LGE: Late gadolinium enhancement; LV: Left ventricle/left ventricular; LVEDV: Left ventricular end-diastolic volume; LVEDV-I: Left ventricular end-diastolic volume index; LVEF: Left ventricular ejection fraction; LVM: Left ventricular mass; LVM-I: Left ventricular mass index; MR: Magnetic resonance; nbh: Non-breathhold (free breathing); PSIR: Phase-sensitive inversion recovery; ROI: Region-of-interest; RV: Right ventricle/right ventricular; SD: Standard deviation; SNR: Signal-to-noise ratio; SR: Sinus rhythm; STRM: Semi-automated signal threshold versus reference mean; SV-I: Stroke volume index; TE: Echo time; TI: Inversion time

Acknowledgements

We sincerely acknowledge the support of our CMR technicians Denise Kleindienst, Kerstin Kretschel and Evelyn Polzin as well as our study nurses Annette Köhler-Rohde and Elke Nickel-Szczech in conducting all study scans. We sincerely thank Carsten Schwenke PhD for his continuous support in matters of study statistics and power calculation throughout this study. We also acknowledge the help of Johannes Kuttner during internal manuscript review.

Consent for study participation

Study individuals have given their written consent for participating in this study.

Funding

No external funding has been received for the realization of this study.

Availability of data and materials

The datasets analyzed during the current study are available from the corresponding author upon reasonable request. Original imaging data are not publicly available due to lawful data protection in Germany.

Authors' contributions
FM developed study design, applied for ethic board approval, conducted major part of CMR scans, led image analysis and data interpretation and was the major contributor in writing the manuscript. KA conducted major parts of image analysis and statistical data interpretation. SiF was involved in image analysis and manuscript writing. StF was involved in image analysis and manuscript writing. MP conducted CMR scans and was involved in image analysis. JK was involved in image analysis and manuscript writing. LZ was involved in data analysis and manuscript writing. FK was involved in data analysis and manuscript writing. JS supervised overall study design, ensured quality control on image analysis and data interpretation, supervised manuscript writing and provided continuous guidance throughout study realization as head of the working group. All authors have read and approved the final manuscript.

Ethics approval and consent to participate
The study was approved by Charité University Medicine ethics board at Charité Campus Mitte, Berlin, Germany.

Consent for publication
Individuals have given their written consent for anonymous publication.

Competing interests
The authors declare that they have no competing interests.

Publisher's Note

Author details
[1]Working Group on Cardiovascular Magnetic Resonance, Experimental and Clinical Research Center - a joint cooperation between the Charité Medical Faculty and the Max-Delbrück Center for Molecular Medicine and HELIOS Hospital Berlin-Buch, Department of Cardiology and Nephrology, Lindenberger Weg 80, 13125 Berlin, Germany. [2]Clinic Agatharied, Department of Cardiology, Ludwig-Maximilians-University Munich, Norbert-Kerkel-Platz, 83734, Hausham, Germany.

Received: 10 July 2017 Accepted: 5 February 2018
Published online: 19 February 2018

References
1. Kim RJ, Wu E, Rafael a, Chen EL, Parker MA, Simonetti O, Klocke FJ, Bonow RO, Judd RM. the use of contrast-enhanced magnetic resonance imaging to identify reversible myocardial dysfunction. N Engl J Med. 2000;343(20):1445–53.
2. Saeed M, Weber O, Lee R, Do L, Martin A, Saloner D, Ursell P, Robert P, Corot C, Higgins CB. Discrimination of myocardial acute and chronic (scar) infarctions on delayed contrast enhanced magnetic resonance imaging with intravascular magnetic resonance contrast media. J Am Coll Cardiol. 2006;48(10):1961–8.
3. Bondarenko O, Beek AM, Nijveldt R, McCann GP, van Dockum WG, Hofman MB, Twisk JW, Visser CA, van Rossum AC. Functional outcome after revascularization in patients with chronic ischemic heart disease: a quantitative late gadolinium enhancement CMR study evaluating transmural scar extent, wall thickness and periprocedural necrosis. Journal of cardiovascular magnetic resonance : official journal of the Society for Cardiovascular Magnetic Resonance. 2007;9(5):815–21.
4. Fluechter S, Kuschyk J, Wolpert C, Doesch C, Veltmann C, Haghi D, Schoenberg SO, Sueselbeck T, Germans T, Streitner F, et al. Extent of late gadolinium enhancement detected by cardiovascular magnetic resonance correlates with the inducibility of ventricular tachyarrhythmia in hypertrophic cardiomyopathy. Journal of cardiovascular magnetic resonance : official journal of the Society for Cardiovascular Magnetic Resonance. 2010;12:30.
5. Adabag AS, Maron BJ, Appelbaum E, Harrigan CJ, Buros JL, Gibson CM, Lesser JR, Hanna CA, Udelson JE, Manning WJ, et al. Occurrence and frequency of arrhythmias in hypertrophic cardiomyopathy in relation to delayed enhancement on cardiovascular magnetic resonance. J Am Coll Cardiol. 2008;51(14):1369–74.
6. Ise T, Hasegawa T, Morita Y, Yamada N, Funada A, Takahama H, Amaki M, Kanzaki H, Okamura H, Kamakura S, et al. Extensive late gadolinium enhancement on cardiovascular magnetic resonance predicts adverse outcomes and lack of improvement in LV function after steroid therapy in cardiac sarcoidosis. Heart. 2014;100(15):1165–72.
7. Neilan TG, Shah RV, Abbasi SA, Farhad H, Groarke JD, Dodson JA, Coelho-Filho O, McMullan CJ, Heydari B, Michaud GF, et al. The incidence, pattern, and prognostic value of left ventricular myocardial scar by late gadolinium enhancement in patients with atrial fibrillation. J Am Coll Cardiol. 2013; 62(23):2205–14.
8. Kramer CM, Barkhausen J, Flamm SD, Kim RJ, Nagel E. Society For cardiovascular magnetic resonance Board of Trustees Task Force on standardized P: standardized cardiovascular magnetic resonance (CMR) protocols 2013 update. Journal of cardiovascular magnetic resonance : official journal of the Society for Cardiovascular Magnetic Resonance. 2013;15:91.
9. von Knobelsdorff-Brenkenhoff F, Schulz-Menger J. Role of cardiovascular magnetic resonance in the guidelines of the European Society of Cardiology. Journal of cardiovascular magnetic resonance : official journal of the Society for Cardiovascular Magnetic Resonance. 2016;18:6.
10. Ponikowski P, Voors AA, Anker SD, Bueno H, Cleland JG, Coats AJ, Falk V, Gonzalez-Juanatey JR, Harjola VP, Jankowska EA, et al. 2016 ESC guidelines for the diagnosis and treatment of acute and chronic heart failure. Revista espanola de cardiologia. 2016;69(12):1167.
11. Kellman P, Arai AE, McVeigh ER, Aletras AH. Phase-sensitive inversion recovery for detecting myocardial infarction using gadolinium-delayed hyperenhancement. *Magnetic resonance in medicine : official journal of the Society of Magnetic Resonance in Medicine / Society of*. Magn Reson Med. 2002;47(2):372–83.
12. Simonetti OP, Kim RJ, Fieno DS, Hillenbrand HB, Wu E, Bundy JM, Finn JP, Judd RM. An improved MR imaging technique for the visualization of myocardial infarction. Radiology. 2001;218(1):215–23.
13. Sievers B, Rehwald WG, Albert TS, Patel MR, Parker MA, Kim RJ, Judd RM. Respiratory motion and cardiac arrhythmia effects on diagnostic accuracy of myocardial delayed-enhanced MR imaging in canines. Radiology. 2008; 247(1):106–14.
14. Muehlberg F, Neumann D, Von Knobelsdorff-Brenkenhoff F, Traber J, Alwardt N, Schulz-Menger J. a multicenter cardiovascular MR network for tele-training and beyond: setup and initial experiences. Journal of the American College of Radiology : JACR. 2015;12(8):876–83.
15. Hendel RC, Friedrich MG, Schulz-Menger J, Zemmrich C, Bengel F, Berman DS, Camici PG, Flamm SD, Le Guludec D, Kim R, et al. CMR first-pass perfusion for suspected inducible myocardial ischemia. JACC Cardiovascular imaging. 2016;9(11):1338–48.
16. Sievers B, Elliott MD, Hurwitz LM, Albert TS, Klem I, Rehwald WG, Parker MA, Judd RM, Kim RJ. Rapid detection of myocardial infarction by subsecond, free-breathing delayed contrast-enhancement cardiovascular magnetic resonance. Circulation. 2007;115(2):236–44.
17. Nguyen TD, Spincemaille P, Weinsaft JW, Ho BY, Cham MD, Prince MR, Wang Y. A fast navigator-gated 3D sequence for delayed enhancement MRI of the myocardium: comparison with breathhold 2D imaging. Journal of magnetic resonance imaging : JMRI. 2008;27(4):802–8.
18. Viallon M, Jacquier A, Rotaru C, Delattre BM, Mewton N, Vincent F, Croisille P. Head-to-head comparison of eight late gadolinium-enhanced cardiac MR (LGE CMR) sequences at 1.5 tesla: from bench to bedside. Journal of magnetic resonance imaging : JMRI. 2011;34(6):1374–87.
19. Morita K, Utsunomiya D, Oda S, Komi M, Namimoto T, Hirai T, Hashida M, Takashio S, Yamamuro M, Yamashita Y. Comparison of 3D phase-sensitive inversion-recovery and 2D inversion-recovery MRI at 3.0 T for the assessment of late gadolinium enhancement in patients with hypertrophic cardiomyopathy. Acad Radiol. 2013;20(6):752–7.
20. Thiele H, Paetsch I, Schnackenburg B, Bornstedt A, Grebe O, Wellnhofer E, Schuler G, Fleck E, Nagel E. Improved accuracy of quantitative assessment of left ventricular volume and ejection fraction by geometric models with steady-state free precession. Journal of cardiovascular magnetic resonance : official journal of the Society for Cardiovascular Magnetic Resonance. 2002; 4(3):327–39.
21. Rudolph A, Messroghli D, Von Knobelsdorff-Brenkenhoff F, Traber J, Schuler J, Wassmuth R, Schulz-Menger J. prospective, randomized comparison of gadopentetate and gadobutrol to assess chronic myocardial infarction applying cardiovascular magnetic resonance. BMC Med Imaging. 2015;15(1):55.

22. Gupta A, Lee VS, Chung YC, Babb JS, Simonetti OP. Myocardial infarction: optimization of inversion times at delayed contrast-enhanced MR imaging. Radiology. 2004;233(3):921–6.
23. Dietrich O, Raya JG, Reeder SB, Reiser MF, Schoenberg SO. Measurement of signal-to-noise ratios in MR images: influence of multichannel coils, parallel imaging, and reconstruction filters. Journal of magnetic resonance imaging : JMRI. 2007;26(2):375–85.
24. Kino A, Zuehlsdorff S, Sheehan JJ, Weale PJ, Carroll TJ, Jerecic R, Carr JC. Three-dimensional phase-sensitive inversion-recovery turbo FLASH sequence for the evaluation of left ventricular myocardial scar. AJR Am J Roentgenol. 2009;193(5):W381–8.
25. Bruder O, Wagner A, Jensen CJ, Schneider S, Ong P, Kispert EM, Nassenstein K, Schlosser T, Sabin GV, Sechtem U, et al. Myocardial scar visualized by cardiovascular magnetic resonance imaging predicts major adverse events in patients with hypertrophic cardiomyopathy. J Am Coll Cardiol. 2010; 56(11):875–87.
26. Rudolph A, Von Knobelsdorff-Brenkenhoff F, Wassmuth R, Prothmann M, Utz W, Schulz-Menger J. assessment of nonischemic fibrosis in hypertrophic cardiomyopathy: comparison of gadopentetate dimeglumine and gadobenate dimeglumine for enhanced cardiovascular magnetic resonance imaging. Journal of magnetic resonance imaging : JMRI. 2014;39(5):1153–60.
27. Mikami Y, Kolman L, Joncas SX, Stirrat J, Scholl D, Rajchl M, Lydell CP, Weeks SG, Howarth AG, White JA. Accuracy and reproducibility of semi-automated late gadolinium enhancement quantification techniques in patients with hypertrophic cardiomyopathy. Journal of cardiovascular magnetic resonance : official journal of the Society for Cardiovascular Magnetic Resonance. 2014;16:85.
28. Messroghli DR, Nordmeyer S, Dietrich T, Dirsch O, Kaschina E, Savvatis K, D oh-I KC, Berger F, Kuehne T. assessment of diffuse myocardial fibrosis in rats using small-animal look-locker inversion recovery T1 mapping. Circulation Cardiovascular imaging. 2011;4(6):636–40.
29. Messroghli DR, Radjenovic A, Kozerke S, Higgins DM, Sivananthan MU, Ridgway JP. Modified look-locker inversion recovery (MOLLI) for high-resolution T1 mapping of the heart. *Magnetic resonance in medicine : official journal of the Society of Magnetic Resonance in Medicine / Society of.* Magn Reson Med. 2004;52(1):141–6.
30. Kellman P, Larson AC, Hsu LY, Chung YC, Simonetti OP, McVeigh ER, Arai AE. Motion-corrected free-breathing delayed enhancement imaging of myocardial infarction. Magn Reson Med. 2005;53(1):194–200.
31. Mikami Y, Cornhill A, Heydari B, Joncas SX, Almehmadi F, Zahrani M, Bokhari M, Stirrat J, Yee R, Merchant N, et al. Objective criteria for septal fibrosis in non-ischemic dilated cardiomyopathy: validation for the prediction of future cardiovascular events. Journal of cardiovascular magnetic resonance : official journal of the Society for Cardiovascular Magnetic Resonance. 2016;18(1):82.
32. Lee SA, Yoon YE, Kim JE, Park JJ, Oh IY, Yoon CH, Suh JW, Kim JS, Chun EJ, Cho YS, et al. Long-term prognostic value of late gadolinium-enhanced magnetic resonance imaging in patients with and without left ventricular dysfunction undergoing coronary artery bypass grafting. Am J Cardiol. 2016; 118(11):1647–54.
33. Hulten E, Agarwal V, Cahill M, Cole G, Vita T, Parrish S, Bittencourt MS, Murthy VL, Kwong R, Di Carli MF, et al. Presence of late gadolinium enhancement by cardiac magnetic resonance among patients with suspected cardiac sarcoidosis is associated with adverse cardiovascular prognosis: a systematic review and meta-analysis. Circulation Cardiovascular imaging. 2016;9(9):e005001.
34. Chan RH, Maron BJ, Olivotto I, Pencina MJ, Assenza GE, Haas T, Lesser JR, Gruner C, Crean AM, Rakowski H, et al. Prognostic value of quantitative contrast-enhanced cardiovascular magnetic resonance for the evaluation of sudden death risk in patients with hypertrophic cardiomyopathy. Circulation. 2014;130(6):484–95.
35. Grun S, Schumm J, Greulich S, Wagner A, Schneider S, Bruder O, Kispert EM, Hill S, Ong P, Klingel K, et al. Long-term follow-up of biopsy-proven viral myocarditis: predictors of mortality and incomplete recovery. J Am Coll Cardiol. 2012;59(18):1604–15.
36. Friedrich MG, Sechtem U, Schulz-Menger J, Holmvang G, Alakija P, Cooper LT, White JA, Abdel-Aty H, Gutberlet M, Prasad S, et al. Cardiovascular magnetic resonance in myocarditis: a JACC white paper. J Am Coll Cardiol. 2009;53(17):1475–87.
37. Knowles BR, Caulfield D, Cooklin M, Rinaldi CA, Gill J, Bostock J, Razavi R, Schaeffter T, Rhode KS. 3-D visualization of acute RF ablation lesions using MRI for the simultaneous determination of the patterns of necrosis and edema. IEEE Trans Biomed Eng. 2010;57(6):1467–75.
38. Weingartner S, Akcakaya M, Basha T, Kissinger KV, Goddu B, Berg S, Manning WJ, Nezafat R. Combined saturation/inversion recovery sequences for improved evaluation of scar and diffuse fibrosis in patients with arrhythmia or heart rate variability. Magn Reson Med. 2014;71(3):1024–34.
39. Rinck PA, Muller RN. Field strength and dose dependence of contrast enhancement by gadolinium-based MR contrast agents. Eur Radiol. 1999; 9(5):998–1004.
40. Kido T, Kido T, Nakamura M, Kawaguchi N, Nishiyama Y, Ogimoto A, Miyagawa M, Mochizuki T. Three-dimensional phase-sensitive inversion recovery sequencing in the evaluation of left ventricular myocardial scars in ischemic and non-ischemic cardiomyopathy: comparison to three-dimensional inversion recovery sequencing. Eur J Radiol. 2014;83(12):2159–66.
41. Morsbach F, Gordic S, Gruner C, Niemann M, Goetti R, Gotschy A, Kozerke S, Alkadhi H, Manka R. Quantitative comparison of 2D and 3D late gadolinium enhancement MR imaging in patients with Fabry disease and hypertrophic cardiomyopathy. Int J Cardiol. 2016;217:167–73.
42. Keegan J, Gatehouse PD, Haldar S, Wage R, Babu-Narayan SV, Firmin DN. Dynamic inversion time for improved 3D late gadolinium enhancement imaging in patients with atrial fibrillation. *Magnetic resonance in medicine : official journal of the Society of Magnetic Resonance in Medicine / Society of.* Magn Reson Med. 2015;73(2):646–54.
43. Kellman P, Xue H, Olivieri LJ, Cross RR, Grant EK, Fontana M, Ugander M, Moon JC, Hansen MS. Dark blood late enhancement imaging. Journal of cardiovascular magnetic resonance : official journal of the Society for Cardiovascular Magnetic Resonance. 2016;18(1):77.

ESC HEART FAILURE
ESC Heart Failure (2018)
Published online in Wiley Online Library (wileyonlinelibrary.com) **DOI:** 10.1002/ehf2.12277

ORIGINAL RESEARCH ARTICLE

Native myocardial T1 time can predict development of subsequent anthracycline-induced cardiomyopathy

Fabian Muehlberg[1,2]*, Stephanie Funk[1,2], Leonora Zange[1,2], Florian von Knobelsdorff-Brenkenhoff[1,2,3], Edyta Blaszczyk[1,2], Alexander Schulz[1,2], Saeed Ghani[4], Annete Reichardt[4], Peter Reichardt[4] and Jeanette Schulz-Menger[1,2]

[1]*Working Group on Cardiovascular Magnetic Resonance, Experimental and Clinical Research Center – a joint cooperation between the Charité Medical Faculty and the Max-Delbrück Center for Molecular MedicineBerlin, Germany;* [2]*Department of Cardiology and Nephrology, HELIOS Hospital Berlin-Buch, Berlin, Germany;* [3]*Clinic Agatharied, Department of Cardiology, Ludwig-Maximilian University of Munich, Hausham, Germany;* [4]*Department for Interdisciplinary Oncology and Sarcoma Center, HELIOS Hospital Berlin-Buch, Berlin, Germany*

Abstract

Aims This study aims to assess subclinical changes in functional and morphological myocardial magnetic resonance parameters very early into an anthracycline treatment, which may predict subsequent development of anthracycline-induced cardiomyopathy (aCMP).

Methods and results Thirty sarcoma patients with planned anthracycline-based chemotherapy (360–400 mg/m^2 doxorubicin-equivalent) were recruited. Median treatment time was 19.1 ± 2.1 weeks. Enrolled individuals received three cardiovascular magnetic resonance studies (before treatment, 48 h after first anthracycline treatment, and upon completion of treatment). Native T1 mapping (modified Look–Locker inversion recovery 5s(3s)3s), T2 mapping, and extracellular volume maps were acquired in addition to a conventional cardiovascular magnetic resonance with steady-state free precession cine imaging at 1.5 T. Patients were given 0.2 mmol/kg gadoteridol for extracellular volume quantification and late gadolinium enhancement imaging. Development of relevant aCMP was defined as drop of left ventricular ejection fraction (LVEF) by >10%. For analysis, 23 complete data sets were available. Nine patients developed aCMP with LVEF reduction >10% until end of chemotherapy. Baseline LVEF was not different between patients with and without subsequent aCMP. When assessed 48 h after first dose of antracyclines, patients with subsequent aCMP had significantly lower native myocardial T1 times compared with before therapy (1002.0 ± 37.9 vs. 956.5 ± 29.2 ms, $P < 0.01$) than patients who did not develop aCMP (990.9 ± 56.4 vs. 978.4 ± 57.4 ms, $P > 0.05$). Patients with aCMP had decreased left ventricular mass upon completion of therapy (86.9 ± 24.5 vs. 81.1 ± 22.3 g; $P = 0.02$), while patients without aCMP did not show a change in left ventricular mass (81.8 ± 21.0 vs. 79.2 ± 18.1 g; $P > 0.05$). No patient developed new myocardial scars or compact myocardial fibrosis under chemotherapy.

Conclusions Early decrease of T1 times 48 h after first treatment with anthracyclines can predict the development of subsequent aCMP after completion of chemotherapy.

Keywords Anthracyclines; Cardiomyopathy; T1 mapping; Cardiac MR; Cardiovascular MR; Cardiotoxicity

Received: 11 December 2017; Revised: 19 January 2018; Accepted: 30 January 2018
**Correspondence to: Fabian Muehlberg, Working Group on Cardiovascular Magnetic Resonance, Experimental and Clinical Research Center – a joint cooperation between the Charité Medical Faculty and the Max-Delbrück Center for Molecular Medicine and Department of Cardiology and Nephrology, HELIOS Hospital Berlin-Buch, Berlin, Germany. Email: fabian.muehlberg@helios-gesundheit.de*

Introduction

Anthracyclines are the mainstay of treatment in many malignancies. Approximately 32% of all breast cancer patients,[1] 60% of elderly lymphoma patients, and most soft tissue sarcoma patients receive anthracyclines during the course of their oncological treatment.[2]

As outcomes of most cancer patients significantly improved over the last decades, the number of cancer survivors has drastically increased.[3]

This fortunate development leads to a progressive importance of long-term side effects of chemotherapy.

Anthracyclines are known to frequently have cardiotoxic side effects. Heart failure due to anthracyclines has severe

prognostic implications as it can lead to mortality rates worse than that associated with many malignancies.[4]

The overall incidence of cardiotoxicity, defined as a reduction in left ventricular ejection fraction (LVEF) of >10%, has been reported in up to 30% of patients receiving anthracyclines.[5]

While the exact mechanism of cardiotoxicity has not been fully understood yet, studies have shown that oxidative tissue injury from free radicals, impaired protein synthesis, and altered calcium handling in cardiomyocytes contribute to its development.[6,7]

There is empirical evidence for the existence of risk factors increasing the likelihood of cardiac dysfunction due to anthracyclines, that is age, known cardiovascular disease, dosage and bolus application.[8]

However, until now, there is no tool for prediction of cardiotoxicity before or early in the treatment. Hence, clinical guidelines and consensus statements of major cardiology and oncology societies on prevention and treatment of anthracycline-induced cardiomyopathy (aCMP) concentrate on serial screening for LVEF reduction before, during, and after chemotherapy.[9,10]

Cardiovascular magnetic resonance (CMR) is a non-invasive imaging technique that allows thorough myocardial tissue differentiation. Myocardial T1 and T2 mapping are promising techniques in this regard as they enable quantitative assessment of diffuse myocardial tissue alteration through a pixel-wise analysis approach.[11,12]

Several studies with animals and human cancer survivors revealed that anthracycline therapy can induce diffuse myocardial fibrosis several years after completion of treatment, which can be assessed by T1 mapping.[13,14]

While myocardial fibrosis is well known to be associated with increased risk for development of congestive heart failure and worse patient outcome, it can only be detected late into or after completion of chemotherapy and, hence, has no substantial preventive benefit for patients receiving anthracyclines.[15,16]

Early preclinical detection of patients with aCMP could lead to a benefit of earlier treatment, thus enabling patients to receive full chemotherapy with lower risk for development of aCMP.[17]

Until today, there is no single universally accepted definition or categorization of cardiotoxicity by anthracyclines. There are several types of aCMP that are categorized according to timing of onset of cardiac dysfunction into acute (days after start of chemotherapy), early-onset (months after start of chemotherapy), and late-onset aCMP (years after completion of chemotherapy).[18] In this study, we focused on development of early-onset aCMP.

We hypothesized that cardiotoxicity of anthracyclines affects cardiac tissue morphology already very early into the treatment and that these alterations may be detected by CMR. Accordingly, the purpose of this study was to assess the predictive value of parametric mapping techniques for detection of acute effects of anthracyclines on cardiac tissue at the beginning of treatment, which may lead to reduction in LVEF after completion of treatment.

Methods

Study population

A total of 30 patients were prospectively recruited. All patients had histologically confirmed soft tissue sarcoma and were planned for anthracycline-based chemotherapy with a cumulative doxorubicin-equivalent dose of 360–400 mg/m^2. Exclusion criteria were chronic renal failure (glomerular filtration rate < 30 mL/m^2), cardiac metastases, previous treatment with anthracyclines, known incompatibility for gadolinium contrast media, and contraindication for magnetic resonance imaging. All enrolled individuals were approved by the local ethical review board and gave written informed consent before participation.

Cardiovascular magnetic resonance protocol

All study participants underwent three CMR scans of 45 min each on a 1.5 T Siemens AvantoFit® scanner (Siemens Healthineers, Erlangen, Germany) with a 32 channel phased array coil. The first CMR scan was performed within 48 h before start of anthracycline treatment (baseline CMR), the second scan 48 h after the first anthracycline treatment, and the third scan 4 weeks after the last anthracycline treatment (usually 5 to 6 months after begin of therapy). Participants received 0.2 mmol/kg of gadoteridol contrast agent (ProHance®, Bracco Diagnostics, Princeton, New Jersey) during each scan. All imaging sequences were performed according to previously published techniques. Left ventricular (LV) and right ventricular (RV) volumetric and functional parameters were assessed in long-axis and short-axis steady-state free precession cine sequences. Cine imaging parameters included field of view (FOV) 340 mm, voxel size 1.8 × 1.8 × 7 mm^3, 3 mm gap, echo time (TE) 1.2 ms, repetition time (TR) 33.4 ms, flip angle 74°, and bandwidth 930 Hz.

T1 mapping was performed using a modified Look–Locker inversion recovery sequence in a mid-ventricular short-axis slice before and 15 min after contrast administration. Sequence parameters include native T1: 5s(3s)3s with FOV 360 mm, voxel size 1.6 × 1.6 × 7 mm^3, TE 1 ms, TR 339.4 ms, flip angle 35°, and bandwidth 1063 Hz and post-contrast: 4s(1s)3s (1s)2s with FOV 360 mm, voxel size 1.6 × 1.6 × 7 mm^3, TE 1 ms, TR 419.4 ms, flip angle 35°, and bandwidth 1063 Hz.

Motion-corrected T2 mapping was performed using an established T2 prepared steady-state free precession technique (3 single-shot images with T2 preparation times of 0/24/55 ms and voxel size of 1.6 × 1.6 × 6.0 mm).[19]

Late gadolinium enhancement (LGE) was used for focal fibrosis imaging and performed in the same slice positions as cine imaging using a gradient echo-based segmented phase-sensitive inversion recovery sequence in single-slice, single-breathhold fashion. LGE scan parameters: FOV 380 mm, voxel size 1.8 × 1.8 × 7 mm, no interslice gap, TE 1 ms, TR 700 ms, flip angle 65°, and bandwidth 1184 Hz.

Image analysis

Experienced readers (F. M., S. F., L. Z., and A. S.) with at least 3 years of experience in cardiac MR analysis in a centre with 3.000 scans per year were blinded to clinical patient information. All image analysis was performed using cvi42® post-processing software version 4.2 (Circle Cardiovascular Imaging Inc., Calgary, Canada). LV and RV size and function as well as LV mass were assessed in short-axis cine images, and atrial volumes were assessed monoplanar (right atrium) or biplanar (left atrium) in long-axis cine four-chamber and two-chamber views.

Epicardial and endocardial contours in a mid-ventricular short-axis slice were traced for T1 and T2 mapping analyses and a 5% safety margin was applied endocardial and epicardial to minimize partial volume effects. Both T2 and T1 maps were quantified as average global values in the analysed slice as previously reported.[19] Visual surveys were evaluated for artefacts before quantification, and segments with relevant artefacts were excluded from analysis (e.g. caused by susceptibility, unintended motion effects, or incorrect motion correction).

Relative and absolute extracellular volume (ECV) fraction were calculated by means of native and post-contrast T1 values and haematocrit as previously established.[12] Relative ECV was reported as per cent of myocardial volume of the corresponding short-axis plane, and absolute ECV in gram extrapolated towards LV mass.

Visual evaluation of LGE images was performed by two independent readers and included presence, location, and transmurality of identified lesions. Differentiation of real LGE lesions from artefacts was realized during image acquisition by verification in two perpendicular slices or altered readout direction.

Interobserver and intraobserver variability analysis was performed on subsets of 10 subjects.

According to current guidelines, patients with LVEF drop of $>$10% points were defined as patients with aCMP. All other patients were defined non-aCMP patients for further analysis.

Laboratory blood analysis

On the day of each CMR scan, venous blood samples were obtained and immediately sent for laboratory analysis at our central laboratory. High-sensitivity cardiac troponin T concentrations were measured using the Elecsys® hsTNT STAT assay (Roche Diagnostics, Mannheim, Germany). The analytical limit of detection was 5 ng/L, and the 99th percentile upper reference limit was 14 ng/L.

Plasma N terminal pro brain natriuretic peptide (NT-proBNP) concentrations were measured using the Elecsys® proBNP II assay (Roche Diagnostics). The analytical limit of detection of NT-proBNP was 5 pg/mL.

Electrocardiography

A 12 lead electrocardiography (ECG) was obtained before each CMR scan and assessed for pathological findings. In detail, patients were ranked positive if one of the following criteria was newly present: no sinus rhythm, PQ interval of $\geq$200 ms, QRS duration of $\geq$120 ms, and atrioventricular blockage, elevation, or depression of ST interval $>$ 0.1 mV. 30.

Statistical analysis

All measured values are shown as mean ± standard deviation. Statistical analysis was performed using SPSS Statistics 22.0.0 (IBM, Armonk, NY, USA). Using Wilcoxon signed-rank test, significant values were accepted by $P < 0.05$.

Univariate analysis for prediction of LVEF drop was performed using two-sided *t*-test embedded into ANOVA analysis.

Correlation analyses were performed using the Spearman rank correlation coefficients. To test for group-differences of categorical variables χ^2-test was applied.

For intraobserver and interobserver reproducibility, images were analysed twice by blinded readers. The results were evaluated by intraclass correlation coefficients.

Results

Patient characteristics

We initially recruited 30 patients. Seven individuals had to be excluded because of early study abort because of individual wish (n = 2) or termination of anthracycline chemotherapy during the study (n = 5). Finally, we had 23 data sets for analysis. Mean age of study cohort was 58.7 ± 13.4 years; 12 patients (52%) were female. Baseline characteristics of study cohort are summarized in *Table 1*. Patients received a mean cumulative dose of doxorubicin-equivalent chemotherapy of

Table 1 Patient characteristics

Patient characteristics	
Age	58.7 ± 13.4 years
Gender	11 M/12 F
BMI	23.5 ± 3.4 kg/m^2
Hypertension	11/23 (48%)
Diabetes	3/23 (13%)
CAD	1/23 (4%)
(Ex-) Smoker	5/23 (22%)

BMI, body mass index; CAD, coronary artery disease.

342 ± 23 mg/m^2 within a mean treatment time of 19.1 ± 2.1 weeks.

Left ventricular and right ventricular function

At the end of chemotherapy, nine patients had developed LVEF reduction >10% as compared with baseline and were defined as aCMP patients for further analysis. See *Figure 1A,B* for representative example. In this aCMP group mean, LVEF decreased from 63.5% ± 5.8% at baseline to 49.9% ± 5.0% after chemotherapy ($P < 0.01$), whereas the remaining 14 non-aCMP patients had no difference in LVEF until completion of therapy (baseline: 59.2% ± 10.3%; after chemotherapy: 58.3 ± 7.8%; $P = 0.47$). Individual LVEF changes between baseline and completion of chemotherapy are displayed in *Figure 2*, and detailed results of anatomical and functional parameters of all CMR studies are illustrated in *Table 2A*. Notably, in aCMP patients, LV mass decreased from baseline (86.9 ± 24.5 g) until completion of therapy (81.1 ± 22.3 g; $P = 0.02$), while LV mass did not change in non-aCMP patients over the course of chemotherapy (baseline: 81.8 ± 21.0 g; after therapy: 79.2 ± 18.1 g).

As illustrated in *Table 2A*, at 48 h after the first treatment with anthracyclines, non-aCMP patients showed an increase in LVEF (59.2% ± 10.2% vs. 63.9% ± 7.9%, $P = 0.02$), LV end-diastolic volume (165.1 ± 39.6 vs. 177.5 ± 36.2 mL, $P = 0.03$), and RV ejection fraction (47.3% ± 59.% vs. 51.1% ± 6.2%, $P < 0.01$) as compared with baseline, while patients with subsequent aCMP did not. RV end-diastolic volume and LV mass did not change in either group after the first dose of anthracyclines.

Myocardial tissue differentiation

In patients who developed aCMP, we observed a significant decrease of native T1 times from 1002.0 ± 37.9 ms at baseline to 956.5 ± 29.2 ms at 48 h after the first dose of anthracyclines ($P < 0.01$). Patients without development of aCMP until completion of chemotherapy did not show a significant change in

Figure 1 Representative anthracycline-induced cardiomyopathy imaging data. Steady-state free precession cine imaging captures in diastole and systole (A) before start of chemotherapy [baseline (left ventricular ejection fraction 65%)] and (B) after completion of chemotherapy (left ventricular ejection fraction 45%). (C) Native myocardial T1 maps of patient with anthracycline-induced cardiomyopathy before chemotherapy and 48 h after first dose application. Displayed T1 times were measured as average global left ventricular times in each slice.

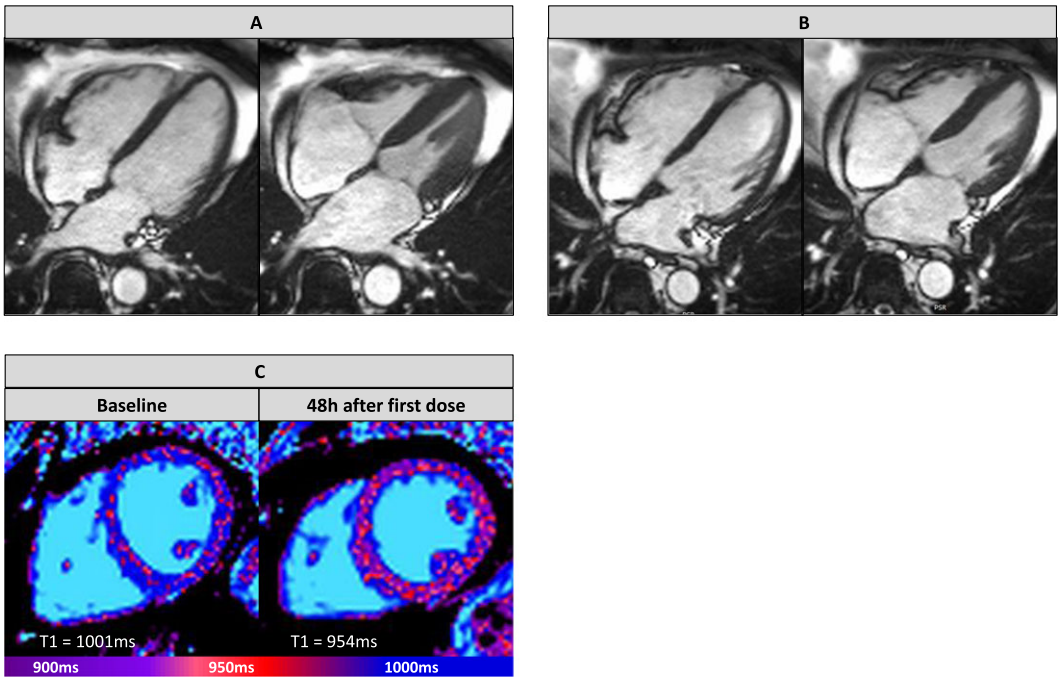

Figure 2 Left ventricular ejection fraction (LVEF) development before and after chemotherapy. Red data points indicate anthracycline-induced cardiomyopathy (aCMP) patients with LVEF drop of >10% during chemotherapy. Averages for aCMP and non-aCMP patients are displayed above.

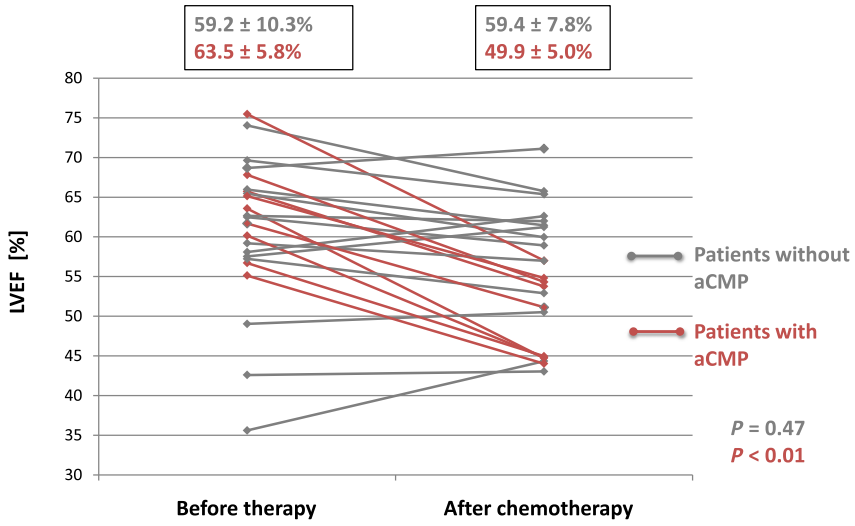

Table 2 Quantitative magnetic resonance parameters. (A) Volumetric and functional assessment. (B) Myocardial tissue differentiation parameters.

				48 h after first dose		After therapy	
			Before therapy		*P* value		*P* value
A							
Non-aCMP	LVEDV	mL	165.1 ± 39.6	**177.5 ± 36.2**	**0.03**	164.7 ± 34.8	0.67
	LVEF	%	59.2 ± 10.2	**63.9 ± 7.9**	**0.02**	58.3 ± 7.8	0.47
	RVEDV	mL	185.7 ± 41.8	196.0 ± 43.0	0.06	184.6 ± 40.7	0.52
	RVEF	%	47.3 ± 5.9	**51.1 ± 6.2**	**<0.01**	47.2 ± 5.8	0.98
	LVM	g	81.8 ± 21.0	81.8 ± 20.1	0.92	79.2 ± 18.1	0.33
aCMP	LVEDV	mL	154.1 ± 32.2	164.3 ± 30.4	0.17	155.8 ± 25.0	0.86
	LVEF	%	63.5 ± 5.8	65.1 ± 4.9	0.34	**49.9 ± 5.0**	**<0.01**
	RVEDV	mL	171.2 ± 36.0	181.6 ± 40.7	0.11	**156.9 ± 33.1**	**<0.01**
	RVEF	%	51.7 ± 3.5	53.3 ± 3.7	0.34	**44.2 ± 5.1**	**<0.01**
	LVM	g	86.9 ± 24.5	85.5 ± 24.6	0.52	**81.1 ± 22.3**	**0.02**
B							
Non-aCMP	T2	ms	52.0 ± 3.5	52.9 ± 2.7	0.07	54.6 ± 3.2	0.08
	Relative ECV	%	26.4 ± 2.0	28.1 ± 2.7	0.12	29.4 ± 1.6	0.06
	Absolute ECV	g	21.0 ± 5.4	23.4 ± 5.8	0.20	23.7 ± 3.9	0.08
aCMP	T2	ms	54.3 ± 2.8	55.3 ± 1.5	0.37	54.8 ± 2.9	0.73
	Relative ECV	%	27.5 ± 2.7	29.3 ± 2.7	0.16	29.8 ± 1.7	0.04
	Absolute ECV	g	23.4 ± 9.2	25.4 ± 8.6	0.33	26.8 ± 4.5	0.15

aCMP, anthracycline-induced cardiomyopathy; LVEF, left ventricular ejection fraction; LVEDV, left ventricular end-diastolic volume; LVM, left ventricular mass; RVEF, left ventricular ejection fraction; RVEDV, right ventricular end-diastolic volume.
P values indicate statistical significance towards baseline data (before therapy).

native T1 at 48 h (990.9 ± 56.4 ms at baseline; 978.4 ± 57.4 ms at 48 h; $P = 0.08$). After completion of therapy, native T1 times were not significantly different from baseline values in either group. For details, see *Figure 3*, a representative imaging example is displayed in *Figure 1C*. Reliability was excellent for both interobserver and intraobserver evaluations (Spearman rank correlation for native T1 times $r_s = 0.90$ with $P = 0.01$ and for T2 times $r_s = 0.91$ with $P = 0.01$, intraclass correlation coefficient 0.96 for native T1 and 0.98 for T2).

Extracellular volume analysis showed that relative and absolute ECV values did not change significantly between baseline and 48 h after first dose of anthracyclines in aCMP and non-aCMP patients (*Table 2B*). Because of the loss in LV mass over the course of chemotherapy, we observed an increase of relative ECV after completion of chemotherapy in aCMP patients against baseline from 27.5% ± 2.7% to 29.8% ± 1.7% ($P = 0.04$). However, this change was not verifiable in absolute ECV values (23.4 ± 9.2 g at baseline vs. 26.8 ± 4.5 g after therapy, $P = 0.15$; for details, see *Table 2B*).

Figure 3 Native T1 mapping. Grey columns represent patients without development of anthracycline-induced cardiomyopathy (aCMP), and red columns represent aCMP patients. *P* values indicate statistical significance towards baseline data (before therapy).

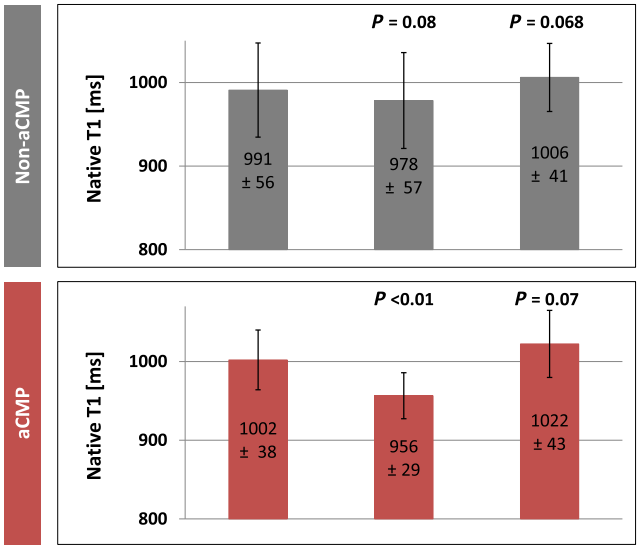

Table 3 Laboratory blood test assessment

			Before therapy	48 hr after first dose		After therapy	
					P value		*P* value
Non-aCMP	High-sensitive troponin T	ng/L	8.1 ± 6.5	8.6 ± 7.0	0.71	**23.3 ± 25.3**	**<0.01**
	NT-proBNP	pg/mL	169.9 ± 160.8	175.0 ± 163.5	0.33	203.0 ± 208.4	0.19
aCMP	High-sensitive troponin T	ng/L	11.4 ± 11.2	11.4 ± 7.2	0.65	**17.7 ± 8.5**	**0.02**
	NT-proBNP	pg/mL	160.7 ± 209.0	169.4 ± 181.2	0.55	265.0 ± 304.7	0.30

aCMP, anthracycline-induced cardiomyopathy; NT-proBNP, N terminal pro brain natriuretic peptide.
P values indicate statistical significance towards baseline data (before therapy).

On evaluation of T2 maps, we did not find focal lesions in any patient at any time point. At baseline, average T2 times were not different between patients with development of subsequent aCMP (54.3 ± 2.8 ms) and non-aCMP patients (52.0 ± 3.5 ms) ($P = 0.11$). Also, on follow-up at 48 h and after completion of therapy, average T2 times did not significantly change in either patient group. For details, see *Table 2B*.

LGE analysis revealed that three patients had myocardial fibrosis at baseline CMR. Two of these three subjects were in the non-aCMP group and had minor subendocardial scars as well as known coronary artery disease. One individual was in the aCMP group and had a small intramyocardial fibrosis inferolateral. None of the detected LGE lesions changed on both follow-up CMR scans. No patient developed new LGE lesions over the course of this study.

Laboratory results

High-sensitive troponin T and NT-proBNP blood analysis are displayed in *Table 3*. There was no significant difference in troponin T levels at baseline between aCMP (11.4 ± 11.2 ng/L) and non-aCMP patients (8.1 ± 6.5 ng/L) and no significant change at 48 h after first anthracycline treatment (aCMP: 11.4 ± 7.2 ng/L; non-aCMP: 8.6 ± 7.0 ng/L). However, upon completion of study, we observed an increase of troponin T levels against baseline in both patient groups (aCMP: 17.7 ± 8.5 ng/L – $P = 0.04$; non-aCMP: 23.3 ± 25.3 ng/L – $P < 0.01$). NT-proBNP was neither different between aCMP and non-aCMP patients at any time point nor did we see a statistically significant increase at 48 h or upon completion of chemotherapy (*Table 3*). Glomerular filtration rates did not significantly change in aCMP (baseline: 87.8 ± 14.1 mL/min/1.73 m^2; at 48 h: 91.1 ± 16.5 mL/min/1.73 m^2; after chemotherapy: 90.8 ± 13.6 mL/min/1.73 m^2, $P > 0.05$) and non-aCMP patients (baseline: 88.1 ± 18.0 mL/min/1.73 m^2; at 48 h: 91.8 ± 19.1 mL/min/1.73 m^2; after chemotherapy: 93.9 ± 20.3 mL/min/1.73 m^2, $P > 0.05$) over the course of the study.

Conduction abnormalities

We found ECG abnormalities only in three patients, two of which were in the aCMP group. One aCMP patient had first

degree atrioventricular blockage after completion of therapy, which was not present at baseline. In the other aCMP patient, we detected atrial fibrillation after chemotherapy but normal sinus rhythm at baseline and at 48 h after therapy start. One non-aCMP patient had complete LV branch block at baseline, which was persistent on follow-up ECGs.

Discussion

In this study, we were able to detect several myocardial tissue changes predicting an early-onset cardiomyopathy because of anthracyclines. Firstly, 30% of recruited patients showed a decrease in LVEF of more than 10% over the course of an anthracycline-based chemotherapy, which was defined as development of aCMP. Secondly, all patients who develop aCMP (30% of recruited patients) had decreased LV mass upon completion of therapy, while patients without aCMP did not show a change in LV mass. Thirdly, a decrease of native myocardial T1 time within 48 h after the first dose of anthracyclines was associated with subsequent development of aCMP. This acute decrease in native T1 time resolved in all aCMP patients until completion of therapy. Finally, myocardial T2 mapping, absolute ECV values, and blood biomarkers did not qualify to discriminate between patients with and without development of aCMP in this study.

The prevalence of aCMP has been shown to be 3% to 48% depending on several variables.[5,20,21] Besides the cumulative dose of anthracyclines administered being one major risk factor for aCMP, there is evidence that the type of imaging modality for LVEF evaluation impacts detection rates for aCMP. CMR is widely accepted as the reference method for measurement of LV volumes and LVEF because of best reproducibility among non-invasive imaging techniques.[22,23]

In several studies, CMR was shown to be superior to echocardiography in detection of LVEF decline under anthracycline therapy, that is revealing an LVEF drop to $<$50% in 26% of all patients within 6 months of therapy using CMR, which is in line with our results.[23,24]

Our finding that patients with aCMP show a reduction of LV mass over the course of chemotherapy is in line with previous limited data on anthracyclines as well as trastuzumab therapy.[25]

Lipshultz *et al*. performed serial echocardiography on children receiving anthracyclines. They found that LV decreased over time under anthracycline therapy and that the reduction in LV mass was inversely related to cumulative dose of anthracyclines.[26]

Because patients in this study received similar cumulative dose of anthracyclines independent of development of aCMP, the dosing factor should play a minor role in our cohort.

Myocardial atrophy and cachexia are known to be independent predictors for mortality in cancer patients.[27] The decrease of LV mass in patients with aCMP in this study shows that myocardial atrophy may also serve as phenotypic criterion for aCMP. However, it is difficult to say if LV atrophy is cause or consequence of aCMP.

Myocardial T1 and T2 mapping, including the derived ECV, are recognized as potential biomarkers of chemotherapy cardiotoxicity that may have the ability to detect myocardial tissue damage earlier than conventional functional metrics. Several CMR studies with cancer survivors have investigated changes in native myocardial T1 and T2 times and found that anthracyclines can cause an increase of native T1 times and ECV because of development of diffuse myocardial fibrosis years after completion of treatment.[14,28]

Hence, there clearly is a long-term myocardial remodelling effect because of anthracyclines, which increases risk for cardiovascular disease.

In this study, we demonstrated evidence that an early decrease of native myocardial T1 time after the first administration of anthracyclines is linked to subsequent development of aCMP, allowing for very early identification of patients at high risk for aCMP.

The pathophysiologic mechanism behind this decrease in native T1, however, remains unclear. There is a lack of previous histologic or imaging data at this early timing of myocardial tissue assessment after drug administration.

In an earlier study from our group, we reported that changes in early myocardial enhancement after gadolinium administration can predict LVEF drop after 28 days in patients treated with anthracyclines.[29] However, there was no longer follow-up of patients.

One hypothesis includes the involvement of radical oxygen species, which are known to play a key role in anthracycline-mediated cardiotoxicity and which affect mitochondrial function and increase lipid peroxidation.[30]

Native T1 time is increased in case of myocardial oedema or inflammation and decreased by iron overload such as in haemochromatosis or in case of lipid deposition as in Fabry disease.[31]

While it is unlikely that a temporary myocardial iron overload is triggered by anthracyclines, they may lead to an increase of intracellular lipid contents affecting native myocardial T1 times.

Other acute anthracycline-meditated biochemical abnormalities in cardiomyocytes may also play a role in the observed decrease of native T1 times.

Our observation that T1 times normalize again upon completion of therapy further strengthen the possibility that acute toxic effects are meditating the early native T1 decrease rather than permanent structural changes such as interstitial fibrosis.

This is supported by our finding that absolute ECV values did not change in our study population—neither acutely after the first administration of anthracyclines nor upon completion of therapy. Other groups have reported that there is increase in relative ECV because of anthracyclines, which may occur even years after therapy.[14]

In our opinion, there certainly is a degree of increased fibrosis attributing to increased relative ECV in the long term. However, the reduction of LV mass during and after cancer therapy due to weight loss and systemic atrophy may also affect relative ECV values, while absolute ECV values remain largely unaffected as reported in this study.

In our study, we did not find significant changes in myocardial T2 time under and after chemotherapy, which other groups have reported. Farhad *et al*. found increased myocardial T2 times in mice treated with anthracyclines at 5 weeks after beginning of anthracycline treatment, which resolves upon a 20 week follow-up.[32]

In our opinion, timing of imaging is crucial for interpretation of results. Cardiotoxicity of anthracyclines may not translate into a single long-term pathophysiolic mechanism but may rather consist of several phases. Acute toxic effects may lead to early native T1 changes as observed in this study, while chronic myocardial remodelling due to anthracyclines may lead to increased native T1 times and elevated ECV because of diffuse interstitial fibrosis in cancer survivors.

Besides imaging parameters, blood biomarkers have been shown to be altered in patients with aCMP.[33,34]

In our study, we observed significant elevations of high-sensitive troponin T. However, these changes occurred independent of development of aCMP. Troponin T is a sensitive biomarker for myocardial cell death and may therefore be elevated even in patients with minor myocardial damage, which does not lead to systolic heart failure.

NT-proBNP is well established as a biomarker for heart failure, thus maybe elevated in patients developing aCMP. However, in contrast to troponin T, we did not see significant changes of NT-proBNP levels in patients with or without aCMP. This is in line with findings from other groups.[35,36]

In conclusion, native myocardial T1 mapping may represent a suitable tool for aCMP risk stratification very early into the treatment. In contrast to other imaging parameters, it can help to predict aCMP development before functional cardiac impairment occurs. Larger, interventional studies are needed to investigate if preventive measures—such as primary aCMP prevention with beta-blockers or angiotensin-converting enzyme inhibitors—inhibit the early decrease of native T1 times after anthracycline treatment.

Limitations

In this study, we observed patients only until completion of therapy; however, long-term effects of anthracyclines can also develop years after completion of treatment. Studies with longer follow-up may help to discriminate between patients with early-onset and late-onset aCMP.

Acknowledgements

We want to thank or study nurses and MR technicians for their continuous support with data acquisition and recruitment. Special thanks to the entire team of the Department of Interdisciplinary Oncology and Sarcoma Center for their help with patient recruitment.

Conflict of interest

The authors have declared the following potential conflicts of interest (sorted by initials). As members of the cardiac MR working group, F.M., S.F., L.Z., F.V.K.B., E.B., A.S., and J.S.M. received direct or indirect grant support and non-financial support from HELIOS Kliniken GmbH, SIEMENS Healthineers, Bayer Healthcare, and Circle Cardiovascular Imaging. P.R. received personal fees from Bayer Healthcare, Roche, Novartis, Pfizer, Pharma Mar, Clinigen Healthcare, Lilly Deutschland GmbH, Deciphera Pharmaceuticals, Merck, and ARIAD Pharmaceuticals. A.R. and S.G. have no conflicts of interest to declare.

Funding

This work was funded partially by HELIOS Kliniken through HELIOS Research Center grant no. HRC-ID 058429.

References

1. Giordano SH, Lin YL, Kuo YF, Hortobagyi GN, Goodwin JS. Decline in the use of anthracyclines for breast cancer. *J Clin Oncol* 2012; **30**: 2232–2239.
2. Nabhan C, Byrtek M, Rai A, Dawson K, Zhou X, Link BK, Friedberg JW, Zelenetz AD, Maurer MJ, Cerhan JR, Flowers CR. Disease characteristics, treatment patterns, prognosis, outcomes and lymphoma-related mortality in elderly follicular lymphoma in the United States. *Br J Haematol* 2015; **170**: 85–95.
3. Coleman MP, Forman D, Bryant H, Butler J, Rachet B, Maringe C, Nur U, Tracey E, Coory M, Hatcher J, McGahan CE, Turner D, Marrett L, Gjerstorff ML, Johannesen TB, Adolfsson J, Lambe M, Lawrence G, Meechan D, Morris EJ, Middleton R, Steward J, Richards MA, ICBP Module 1 Working Group. Cancer survival in Australia, Canada, Denmark, Norway, Sweden, and the UK, 1995-2007 (the International Cancer Benchmarking Partnership): an analysis of population-based cancer registry data. *Lancet* 2011; **377**: 127–138.
4. Alvarez JA, Russell RR. Cardio-oncology: the Nuclear Option. *Curr Cardiol Rep* 2017; **19**: 31.
5. Swain SM, Whaley FS, Ewer MS. Congestive heart failure in patients treated with

doxorubicin: a retrospective analysis of three trials. *Cancer* 2003; **97**: 2869–2879.
6. Singal PK, Iliskovic N. Doxorubicin-induced cardiomyopathy. *N Engl J Med* 1998; **339**: 900–905.
7. Zhang S, Liu X, Bawa-Khalfe T, Lu LS, Lyu YL, Liu LF, Yeh ET. Identification of the molecular basis of doxorubicin-induced cardiotoxicity. *Nat Med* 2012; **18**: 1639–1642.
8. Cueva JF, Antolin S, Calvo L, Fernandez I, Ramos M, de Paz L, Mata JG, Lopez R, Constenla M, Perez E, González A, Pellón ML, Varela S, López T. Galician consensus on management of cardiotoxicity in breast cancer: risk factors, prevention, and early intervention. *Clin Transl Oncol* 2017; **19**: 1067–1078.
9. Tarantini L, Massimo Gulizia M, Di Lenarda A, Maurea N, Giuseppe Abrignani M, Bisceglia I, Bovelli D, De Gennaro L, Del Sindaco D, Macera F, Parrini I, Radini D, Russo G, Beatrice Scardovi A, Inno A. ANMCO/AIOM/AICO Consensus Document on clinical and management pathways of cardio-oncology: executive summary. *Eur Heart J Suppl* 2017; **19**: D370–D379.
10. Plana JC, Galderisi M, Barac A, Ewer MS, Ky B, Scherrer-Crosbie M, Ganame J, Sebag IA, Agler DA, Badano LP, Banchs J, Cardinale D, Carver J, Cerqueira M, DeCara JM, Edvardsen T, Flamm SD, Force T, Griffin BP, Jerusalem G, Liu JE, Magalhães A, Marwick T, Sanchez LY, Sicari R, Villarraga HR, Lancellotti P. Expert consensus for multimodality imaging evaluation of adult patients during and after cancer therapy: a report from the American Society of Echocardiography and the European Association of Cardiovascular Imaging. *Eur Heart J Cardiovasc Imaging* 2014; **15**: 1063–1093.
11. Kim PK, Hong YJ, Im DJ, Suh YJ, Park CH, Kim JY, Chang S, Lee HJ, Hur J, Kim YJ, Chang S, Lee HJ, Hur J, Kim YJ, Choi BW. Myocardial T1 and T2 mapping: techniques and clinical applications. *Korean J Radiol* 2017; **18**: 113–131.
12. Piechnik SK, Jerosch-Herold M. Myocardial T1 mapping and extracellular volume quantification: an overview of technical and biological confounders. *Int J Cardiovasc Imaging* 2018; **34**: 3–14.
13. Jordan JH, Vasu S, Morgan TM, D'Agostino RB Jr, Melendez GC, Hamilton CA, Arai AE, Liu S, Liu CY, Lima JA, Bluemke DA, Burke GL, Hundley WG. Anthracycline-associated T1 mapping characteristics are elevated independent of the presence of cardiovascular comorbidities in cancer survivors. *Circ Cardiovasc Imaging* 2016; **9**: pii: e004325.
14. Neilan TG, Coelho-Filho OR, Shah RV, Feng JH, Pena-Herrera D, Mandry D, Pierre-Mongeon F, Heydari B, Francis SA, Moslehi J, Kwong RY, Jerosch-Herold M. Myocardial extracellular volume by cardiac magnetic resonance imaging in patients treated with anthracycline-based chemotherapy. *Am J Cardiol* 2013; **111**: 717–722.
15. Schelbert EB, Fridman Y, Wong TC, Abu Daya H, Piehler KM, Kadakkal A, Miller CA, Ugander M, Maanja M, Kellman P, Shah DJ, Abebe KZ, Simon MA, Quarta G, Senni M, Butler J, Diez J, Redfield MM, Gheorghiade M. Temporal relation between myocardial fibrosis and heart failure with preserved ejection fraction: association with baseline disease severity and subsequent outcome. *JAMA Cardiol* 2017; **2**: 995–1006.
16. Yingchoncharoen T, Jellis C, Popovic ZB, Wang L, Gai N, Levy WC, Tang WH, Flamm S, Kwon DH. Focal fibrosis and diffuse fibrosis are predictors of reversed left ventricular remodeling in patients with non-ischemic cardiomyopathy. *Int J Cardiol* 2016; **221**: 498–504.
17. Heck SL, Gulati G, Hoffmann P, von Knobelsdorff-Brenkenhoff F, Storas TH, Ree AH, Gravdehaug B, Rosjo H, Steine K, Geisler J, Schulz–Menger J, Omland T. Effect of candesartan and metoprolol on myocardial tissue composition during anthracycline treatment: the PRADA trial. *Eur Heart J Cardiovasc Imaging* 2017. https://doi.org/10.1093/ehjci/jex159.
18. Levis BE, Binkley PF, Shapiro CL. Cardiotoxic effects of anthracycline-based therapy: what is the evidence and what are the potential harms? *Lancet Oncol* 2017; **18**: e445-e456.
19. Schmacht L, Traber J, Grieben U, Utz W, Dieringer MA, Kellman P, Blaszczyk E, von Knobelsdorff-Brenkenhoff F, Spuler S, Schulz-Menger J. Cardiac involvement in myotonic dystrophy type 2 patients with preserved ejection fraction: detection by cardiovascular magnetic resonance. *Circ Cardiovasc Imaging* 2016; **9**: e004615.
20. Curigliano G, Cardinale D, Dent S, Criscitiello C, Aseyev O, Lenihan D, Cipolla CM. Cardiotoxicity of anticancer treatments: epidemiology, detection, and management. *CA Cancer J Clin* 2016; **66**: 309–325.
21. Krischer JP, Epstein S, Cuthbertson DD, Goorin AM, Epstein ML, Lipshultz SE. Clinical cardiotoxicity following anthracycline treatment for childhood cancer: the Pediatric Oncology Group experience. *J Clin Oncol Off J Am Soc Clin Oncol* 1997; **15**: 1544–1552.
22. Grothues F, Smith GC, Moon JC, Bellenger NG, Collins P, Klein HU, Pennell DJ. Comparison of interstudy reproducibility of cardiovascular magnetic resonance with two-dimensional echocardiography in normal subjects and in patients with heart failure or left ventricular hypertrophy. *Am J Cardiol* 2002; **90**: 29–34.
23. Ylanen K, Eerola A, Vettenranta K, Poutanen T. Three-dimensional echocardiography and cardiac magnetic resonance imaging in the screening of long-term survivors of childhood cancer after cardiotoxic therapy. *Am J Cardiol* 2014; **113**: 1886–1892.
24. Drafts BC, Twomley KM, D'Agostino R Jr, Lawrence J, Avis N, Ellis LR, Thohan V, Jordan J, Melin SA, Torti FM, Little WC, Hamilton CA, Hundley WG. Low to moderate dose anthracycline-based chemotherapy is associated with early noninvasive imaging evidence of subclinical cardiovascular disease. *JACC Cardiovasc Imaging* 2013; **6**: 877–885.
25. Neilan TG, Coelho-Filho OR, Pena-Herrera D, Shah RV, Jerosch-Herold M, Francis SA, Moslehi J, Kwong RY. Left ventricular mass in patients with a cardiomyopathy after treatment with anthracyclines. *Am J Cardiol* 2012; **110**: 1679–1686.
26. Lipshultz SE, Lipsitz SR, Sallan SE, Dalton VM, Mone SM, Gelber RD, Colan SD. Chronic progressive cardiac dysfunction years after doxorubicin therapy for childhood acute lymphoblastic leukemia. *J Clin Oncol* 2005; **23**: 2629–2636.
27. Williams GR, Muss HB, Shachar SS. Cachexia in patients with cancer. *Lancet Oncol* 2016; **17**: e220.
28. Tham EB, Haykowsky MJ, Chow K, Spavor M, Kaneko S, Khoo NS, Pagano JJ, Mackie AS, Thompson RB. Diffuse myocardial fibrosis by T1-mapping in children with subclinical anthracycline cardiotoxicity: relationship to exercise capacity, cumulative dose and remodeling. *J Cardiovasc Magn Reson* 2013; **15**: 48.
29. Wassmuth R, Lentzsch S, Erdbruegger U, Schulz-Menger J, Doerken B, Dietz R, Friedrich MG. Subclinical cardiotoxic effects of anthracyclines as assessed by magnetic resonance imaging-a pilot study. *Am Heart J* 2001; **141**: 1007–1013.
30. Asensio-Lopez MC, Soler F, Pascual-Figal D, Fernandez-Belda F, Lax A. Doxorubicin-induced oxidative stress: The protective effect of nicorandil on HL-1 cardiomyocytes. *PLoS One* 2017; **12**: e0172803.
31. Liu JM, Liu A, Leal J, McMillan F, Francis J, Greiser A, Rider OJ, Myerson S, Neubauer S, Ferreira VM, Piechnik SK. Measurement of myocardial native T1 in cardiovascular diseases and norm in 1291 subjects. *J Cardiovasc Magn Reson* 2017; **19**: 74.
32. Farhad H, Staziaki PV, Addison D, Coelho-Filho OR, Shah RV, Mitchell RN, Szilveszter B, Abbasi SA, Kwong RY, Scherrer-Crosbie M, Hoffmann U, Jerosch–Herold M, Neilan TG. Characterization of the changes in cardiac structure and function in mice treated with anthracyclines using serial cardiac magnetic resonance imaging. *Circ Cardiovasc Imaging* 2016; **9**: e003584.
33. Kitayama H, Kondo T, Sugiyama J, Kurimoto K, Nishino Y, Kawada M, Hirayama M, Tsuji Y. High-sensitive troponin T assay can predict anthracycline- and trastuzumab-induced cardiotoxicity in breast cancer patients. *Breast Cancer* 2017; **24**: 774–782.

34. Cardinale D, Sandri MT, Martinoni A, Borghini E, Civelli M, Lamantia G, Cinieri S, Martinelli G, Fiorentini C, Cipolla CM. Myocardial injury revealed by plasma troponin I in breast cancer treated with high-dose chemotherapy. *Ann Oncol* 2002; **13**: 710–715.
35. Meinardi MT, van Veldhuisen DJ, Gietema JA, Dolsma WV, Boomsma F, van den Berg MP, Volkers C, Haaksma J, de Vries EG, Sleijfer DT, van der Graaf WT. Prospective evaluation of early cardiac damage induced by epirubicin-containing adjuvant chemotherapy and locoregional radiotherapy in breast cancer patients. *J Clin Oncol* 2001; **19**: 2746–2753.
36. Daugaard G, Lassen U, Bie P, Pedersen EB, Jensen KT, Abildgaard U, Hesse B, Kjaer A. Natriuretic peptides in the monitoring of anthracycline induced reduction in left ventricular ejection fraction. *Eur J Heart Fail* 2005; **7**: 87–93.

Mein Lebenslauf wird aus datenschutzrechtlichen Gründen in der elektronischen Version meiner Arbeit nicht veröffentlicht.

Publikationsliste

Artikel in wissenschaftlichen Fachzeitschriften (Peer-Review)

1. Zange L, Muehlberg F, Blaszczyk E, Schwenke S, Traber J, **Funk S,** Schulz-Menger J. Quantification in cardiovascular magnetic resonance: agreement of software from three different vendors on assessment of left ventricular function, 2D flow and parametric mapping. J Cardiovasc Magn Reson. 2019;21(1):12
2. Ma J, März M, **Funk S**, Schulz-Menger J, Kutyniok G, Schaeffter T, Kolbitsch C. Shearlet-based compressed sensing for fast 3D cardiac MR imaging using iterative reweighting. Phys Med Biol. 2018;63(23):235004
3. Muehlberg F, **Funk S**, Zange L, von Knobelsdorff-Brenkenhoff F, Blaszczyk E, Schulz A, Ghani S, Reichardt A, Reichardt P, Schulz-Menger J. Native myocardial T1 time can predict development of subsequent anthracycline-induced cardiomyopathy. ESC Heart Fail. 2018.
4. Muehlberg F, Arnhold K, Fritschi S, **Funk S**, Prothmann M, Kermer J, Zange L, von Knobelsdorff-Brenkenhoff F, Schulz-Menger J. Comparison of fast multi-slice and standard segmented techniques for detection of late gadolinium enhancement in ischemic and non-ischemic cardiomyopathy - a prospective clinical cardiovascular magnetic resonance trial. J Cardiovasc Magn Reson. 2018;20(1):13.
5. **Funk S**, Kermer J, Doganguezel S, Schwenke C, von Knobelsdorff-Brenkenhoff F, Schulz-Menger J. Quantification of the left atrium applying cardiovascular magnetic resonance in clinical routine. Scand Cardiovasc J. 2018;52(2):85-92.
6. Neuner B, von Mackensen S, Holzhauer S, **Funk S**, Klamroth R, Kurnik K, Krumpel A, Halimeh S, Reinke S, Fruhwald M, Nowak-Gottl U. Health-Related Quality of Life in Children and Adolescents with Hereditary Bleeding Disorders and in Children and Adolescents with Stroke: Cross-Sectional Comparison to Siblings and Peers. Biomed Res Int. 2016;2016:1579428.
7. Klein-Weigel PF, Bimmler M, Hempel P, Schopp S, Dreusicke S, Valerius J, Bohlen A, Boehnlein JM, Bestler D, **Funk S**, Elitok S. G-protein coupled receptor auto-antibodies in thromboangiitis obliterans (Buerger's disease) and their removal by immunoadsorption. Vasa. 2014;43(5):347-52.

Vorträge und Poster (wissenschaftliche Kongresse)

1. **Funk S**, Schmitter S, Prothmann M, Schwenke C, von Knobelsdorff-Brenkenhoff F, Greiser A, Bollache E, Markl M, Schulz-Menger J, ”Impact of field strength (1.5, 3.0 and 7.0 Tesla) and sequence on quantification of aortic flow volumes, peak velocity and wall shear stress using 4D flow MRI”, Proc. Intl Soc Magn Reson Med 26, 2018; Paris, France
2. Töpper A, Bhoyroo Y, **Funk S**, Blaszczyk E, Ehrling O, Heisterkamp L, Nickel E, Schulz-Menger J, “Small pericardial and pleural effusions - always a sign for inflammation? A CMR study in healthy females”, Proc. 21th Annual Scientific Sessions Society for Cardiovascular Magnetic Resonance 2018, Barcelona, Spain
3. Kranzusch R, Aus dem Siepen F, **Funk S**, Zange L, Jeuthe S, Ferreira da Silva T, Kühne T, Pieske B, Tillmanns C, Friedrich MG, Schulz-Menger J, Messroghli D, „Z-score scaling for native T1 mapping: Application to normal data from different MR systems and to cardiac amyloidosis“, Proc. 21th Annual Scientific Sessions Society for Cardiovascular Magnetic Resonance 2018, Barcelona, Spain
4. **Funk S**, Muehlberg F, Schmacht L, von Knobelsdorff-Brenkenhoff F, Baberg HT, Schulz-Menger J, “Usage of Cardiovascular Magnetic Resonance in Hospitals of Different Size – Results of the German Multicenter CMR-Network”, Proc. 14th Annual CMR Congress of the European Association of Cardiovascular Imaging (EACVI) of the ESC 2017, Prague, Czech Republic
5. Blaszczyk E, von Knobelsdorff-Brenkenhoff F, **Funk S**, Schmacht L, Grieben U, Kellman P, Spuler S, Schulz-Menger J, Töpper A, “Facioscapulohumeral Muscular Dystrophy (FSHD) – Detection of Fat and Fibrosis in the myocardium in patients with preserved LVEF”, Proc. 20th Annual Scientific Sessions Society for Cardiovascular Magnetic Resonance 2017, Washington D.C., MY, USA
6. Muehlberg F, **Funk S**, Zange L, Schulz A, von Knobelsdorff-Brenkenhoff F, Blaszczyk E, Ghani S, Reichardt A, Schulz-Menger J, “Early changes of native T1 time predict development of subsequent anthracycline-induced cardiomyopathy with impaired systolic function”, Proc. 20th Annual Scientific

Sessions Society for Cardiovascular Magnetic Resonance 2017, Washington D.C., MY, USA

7. Kolbitsch C, Ma J, Schnabel F, Chen Z, **Funk S**, Kutyniok G, Schulz-Menger J, Schaeffter T, “3D High-Resolution LGE MRI using Shearlet-based Compressed-Sensing Image Reconstruction”, Proc. 20th Annual Scientific Sessions Society for Cardiovascular Magnetic Resonance 2017, Washington D.C., MY, USA
8. Zange L, Muehlberg F, **Funk S**, Blaszczyk E, Traber J, Schueler J, Schmacht L, Schulz-Menger J, “Same sequence – different software provider: different results? A post-processing comparison of flow, T1 and T2 mapping”, Proc. 20th Annual Scientific Sessions Society for Cardiovascular Magnetic Resonance 2017, Washington D.C., MY, USA
9. **Funk S**, Kermer J, Dogangüzel S, von Knobelsdorff- Brenkenhoff F, Schulz-Menger J, “Left Atrium assessed by Cardiovascular Magnetic Resonance at 1.5 and 3.0 Tesla – age and gender effects”, Proc. 13th Annual CMR Congress of the European Association of Cardiovascular Imaging (EACVI) of the ESC 2016, Florence, Italy
10. **Funk S**, Kermer J, Dogangüzel S, von Knobelsdorff- Brenkenhoff F, Schulz-Menger J, “Morphologie und Funktion des Linken Vorhofes sind bei Gesunden alters- und geschlechtsabhängig - Normwerte mittels Kardiovaskulärer MRT”, Proc. der 82. Jahrestagung der Deutschen Gesellschaft für Kardiologie- Herz- und Kreislaufforschung 2016, Mannheim, Deutschland
11. Muehlberg F, Arnhold K, **Funk S**, Prothmann M, Rudolph A, von Knobelsdorff-Brenkenhoff F and Schulz-Menger J, „Equivalence of Conventional and Fast Late Gadolinium Enhancement (LGE) Techniques for Quantitative Evaluation of Fibrosis in Ischemic and Non-ischemic Cardiac Disease – Save the Time!”, Proc. 19th Annual Scientific Sessions Society for Cardiovascular Magnetic Resonance 2016, Los Angeles, CA, USA
12. Arnhold K, Muehlberg F, Fritschi S, **Funk S**, Prothmann M, von Knobelsdorff-Brenkenhoff F, Schulz-Menger J, “Equivalence of segmented conventional and fast single-shot late gadolinium enhancement (LGE) techniques for quantitative evaluation of fibrosis in ischemic and non-ischemic cardiac disease”, Proc. 13th Annual CMR Congress of the European Association of Cardiovascular Imaging (EACVI) of the ESC 2016, Florence, Italy

Danksagung

Mein herzlicher Dank gilt allen Probanden, ohne deren Studienteilnahme neue wissenschaftliche Erkenntnisse nicht möglich wären.
Ebenfalls nicht möglich wären diese ohne eine so hervorragende Betreuung junger Wissenschaftler, wie ich sie durch meine Doktormutter Frau Prof. Dr. Jeanette Schulz-Menger erfahren durfte. Sie vermittelte mir durch wertvolle Ratschläge, in unseren anregenden Diskussionen und durch ihre stetige sowohl fachliche als auch menschliche Unterstützung in allen Phasen der Arbeit nicht nur die Begeisterung für diese Arbeit, sondern weckte auch meine Liebe zur weiteren Forschung in diesem Bereich.

Des weiteren möchte ich mich bei allen Koautoren für ihre Unterstützung und die konstruktiven Diskussionen und Anregungen bedanken. Insbesondere gilt mein Dank auch Dr. Fabian Mühlberg für die bereichernde Zusammenarbeit und seine stete Hilfsbereitschaft.
Das gute Arbeitsklima in der gesamten Arbeitsgruppe „Kardiale MRT“ führte zu einer konstruktiven Arbeitsatmosphäre und die hilfreichen Diskussionen in der regelmäßigen Arbeitsgruppentreffen halfen mir oft, neue Blickwinkel zu finden.
Auch möchte ich mich herzlich bei den medizinisch-technischen Röntgenassistentinnen und Studienschwestern für ihr Engagement bei der Durchführung der Untersuchungen bedanken.

Meine Familie und meine Frau unterstützten mich durchgängig liebevoll und gaben mir viel Kraft. Vielen Dank dafür.